

# Newtonian gravitational constant measurement. All atomic variables become extreme when using a source mass consisting of 3 or more parts

B. Dubetsky\*  
 (Dated: April 7, 2020)

Atomic interferometry methods can be used to measure the Newtonian gravitational constant. Due to symmetry factors or purposefully to improve the accuracy, the phase of an atomic interferometer can be measured at extreme values of atomic velocities and coordinates. We propose using a source mass consisting of 3 or more parts, since only in this case one can find such an arrangement of parts that all atomic variables become extreme. Nonlinear dependences of the phase on the uncertainties of atomic positions and velocities near those extreme values required us to modify the expression for the phase relative standard deviation (RSD). Moreover, taking into account nonlinear terms in the phase dependence on the atomic coordinates and velocities leads to a phase shift, which in previous experiments was also not included. A shift of 199 ppm was obtained for the experiment [1]. It reduces the value of Newtonian gravitational constant by 0.02%. In addition, it is shown that at equal sizes of the atomic cloud in the vertical and transverse directions, as well as at equal atomic vertical and transverse temperatures, systematic errors due to the finite size and temperature of the cloud disappear. The calculation also showed that when using the 13-ton source mass proposed in [2], the measurement accuracy can reach 17 ppm for a source mass consisting of 4 quarters. All the consideration was carried out for the source mass consisting of a set of cylinders. An analytical expression for the gravitational field of a homogeneous cylinder is derived.

PACS numbers: 03.75.Dg; 37.25.+k; 04.80.-y

Atom interferometer (AI) [3] is now used to measure Newtonian gravity constant  $G$  [1, 4, 5]. Searches for new schemes and options promise to increase the accuracy of these measurements. Previously, it was shown [6] that, in principle, the current state-of-art in atom interferometry would allow one to measure  $G$  with an accuracy of 200 ppb. To achieve such a goal one has to use *simultaneously* the largest time delay between pulses  $T = 1.15$  s [7], temperature 115 pK and radius of the atom cloud  $170 \mu$  (which are larger than those observed in [8]), the beam splitter with an effective wave vector  $k = 8.25 \cdot 10^8 \text{ m}^{-1}$  [9], the source mass 1080 kg [10] and phase noise  $\phi_{err} = 10^{-4} \text{ rad}$ . For the parameters achieved in [1, 4, 5] at present, the optimal preparation of the atomic clouds and proper positioning of the gravity sources can also lead to an increase in the accuracy of the  $G$ -measurement. According to [2], the main goal here is to reduce the sensitivity of the AI phase to the initial atomic coordinates. Even more important [6, 11] is the sensitivity to the launching atomic velocities.

The following procedure was used [1, 4, 6, 11]. The source mass consists of two halves, which are placed in two different configurations C and F. We accept the notation "C and F," which was previously used in article [1]. The atomic gradiometer [12] measures the phase difference of two atomic interferometers (AIs) 1 and 2

$$\Delta\phi^{(C,F)} = \phi^{(C,F)}(z_1, v_{z_1}) - \phi^{(C,F)}(z_2, v_{z_2}), \quad (1)$$

where  $\phi^{(C,F)}(z_j, v_j)$  is the phase of AI  $j$ , in which the atoms are launched vertically from point  $\mathbf{x}_j = (0, 0, z_j)$

at velocity  $\mathbf{v}_j = (0, 0, v_{z_j})$ . Phase difference (1) consists of two parts, the one that is induced by the gravitational field of the Earth and inertial terms and the other that is associated with the gravitational field of the source mass. One expects [1, 4, 5] that the phase double difference (PDD)

$$\Delta^{(2)}\phi = \Delta\phi^{(C)} - \Delta\phi^{(F)} \quad (2)$$

will depend only on the AI phase  $\phi_s^{(C,F)}(z_j, v_j)$  produced only by the field of source mass, and therefore can be used to measure the Newtonian gravitational constant  $G$ . Despite the fact that the gravitational field of the Earth does not affect the PDD, the gradient of this field affects [1, 4] on the accuracy of the PDD measurement. In the article [1], to reduce this influence, the mutual position of the source mass and atomic clouds are selected so that at the point of apogee of the atomic trajectories gradients of the Earth's field and the field of the source mass cancel each other. Below in Sec. III we will see that this technique only partially reduces the influence of the gravitational field of the Earth on the accuracy of the  $G$  measurement.

A different approach was used in [4]. In the C-configuration, when all the components of the source mass were located between AIs 1 and 2, for a given launching velocity

$$v_{z_1} = v_{z_2} = v, \quad (3)$$

varying the position of the atomic cloud 1, one found the point of the local maximum of the phase  $\phi^{(C)}(z_1, v)$ . Similarly, the cloud of the second interferometer was located at the point of the local minimum of the phase  $\phi^{(C)}(z_2, v_{z_2})$ . In the F-configuration, one varied the

\*Electronic address: bdubetsky@gmail.com

positions of the source mass halves,  $h_1$  and  $h_2$ , in order to achieve a situation, when points  $(z_1, v)$  and  $(z_2, v)$  become respectively the minimum and maximum of the phase  $\phi^{(F)}(z, v)$ . After this procedure, the points  $z_1$  and  $z_2$  become extreme in both the  $C$ - and  $F$ -configurations, and therefore they are extreme for the PDD (2). The disadvantage of this approach is that the atomic velocities  $v_{z_1}$  and  $v_{z_2}$  were not varied and no extreme values were found for them.

To overcome this difficulty, we propose to divide the source mass into a larger number of parts, the position of each of which can vary independently. In the  $C$ -configuration, when all the parts are put together, under a sufficiently strong gravitational field, one can still find the points of local maximum and minimum  $(z_1, v_{z_1})$  and  $(z_2, v_{z_2})$  and place atomic clouds in those points. Our goal is that in the  $F$ -configuration the same points still remain extreme, i.e. they satisfy a system of 4 equations

$$\partial_{z_j} \phi^{(F)}(z_j, v_{z_j}) = \partial_{v_{z_j}} \phi^{(F)}(z_j, v_{z_j}) = 0, \quad (4)$$

where  $j = 1$  or  $2$ . Although the points are given, the phase  $\phi^{(F)}(z, v)$  is a function of the coordinates of the source mass parts, such as their location along the vertical axis,  $h_1, \dots, h_n$ , where  $n$  is the number of parts. Then (4) should be considered as a system of equations for  $(h_1, \dots, h_n)$ . Since the number of equations and the number of variables must coincide, we conclude that the source mass must consist of 4 parts. However, calculations have shown that the extreme values of the velocities of both atomic clouds in the  $C$ -configuration coincide. Therefore, it is sufficient to divide the source mass into 3 parts to make extreme all atomic variables in the both configuration.

To test the feasibility of our proposals, we compared the error budgets in our case and in article [1]. In precision gravity experiments, one calculates or measures the SD  $\sigma$  of the response  $f$  (such as the AI phase or phase difference) using the expression

$$\sigma(f) = \left( \sum_{m=1}^n \sigma_m^2 \right)^{1/2}, \quad (5)$$

where  $n$  is the number of variables  $\{q_1, \dots, q_n\}$ , included in the error budget,  $\sigma_m = |\partial f / \partial q_m| \sigma(q_m)$ , and  $\sigma(q_m)$  is a SD of small uncertainty in the variable  $q_m$ . We assume that variables  $\{q_1, \dots, q_n\}$  are statistically independent. See examples of such budgets in [1, 2, 4, 5, 13]. The situation changes when one considers uncertainties near the extreme points  $\{\mathbf{x}_m, \mathbf{v}_m\}$  and the signal's uncertainty becomes a quadratic function of the uncertainties of the atomic position and velocity  $\{\delta \mathbf{x}_m, \delta \mathbf{v}_m\}$ . There are several examples in which measurements were carried out (or proposed to be carried out) near extreme points. Extreme atomic coordinates were selected in the experiments [4]. Extreme atomic coordinates and velocities were found in the articles [6, 11]. The difficulties of using

extreme points are noted in the article [2], where an alternative approach was proposed, based on the elimination of the dependence of the AI phase on the atomic position and velocity proposed in [14]. However, even in this case, one eliminates only the dependence on the vertical coordinates and velocities, while the transverse coordinates  $\{x_m, y_m\} = \{0, 0\}$  and velocities  $\{v_{x_m}, v_{y_m}\} = \{0, 0\}$  remain extreme. This is because the vertical component of the gravitational field of the hollow cylinder  $\delta g_3(\mathbf{x})$  is axially symmetric, and the expansion of both the field and the field gradient in transverse coordinates begins with quadratic terms. Transverse velocities and coordinates were also extreme in experiment [1]. Since for extreme variables  $\partial f / \partial q_m = 0$ , one sees that in all the cases listed above [1, 2, 4, 6, 11], the use of the expression (5) is unjustified. Revision of this expression is required. Moreover, the quadratic dependence on the uncertainties  $\{\delta \mathbf{x}_m, \delta \mathbf{v}_m\}$  leads to a shift in the signal [19]. Here, we carried out this revision and expressed both the SD and the shift of the PDD (2) in terms of the first and second derivatives of the phases  $\phi^{(C,F)}$  to find contributions to an error budget from both extreme and non-extreme variables.

Recently, we performed [6, 11] calculations, determined the optimal geometry of the gravitational field, positions and velocities of atomic clouds for the source mass of a cuboid shape. The choice of this shape is convenient for calculations since one has an analytical expression for the potential of the cuboid [15]. Despite this, it is preferable to use the source mass in a cylindrical shape to perform high-precision measurements of  $G$  [16]. Cylindrical source masses were used to measure  $G$  in [1, 4]. The hollow cylinder source mass has been proposed to achieve an accuracy of 10ppm [2]. The analytical expression for the gravitational field along the  $z$ -axis of the hollow cylinder was explored [2], but outside this axis, the potential expansion into spherical harmonics was used [1, 4]. Expressions for the field of the cylinders have been derived in the articles [17, 18]. Alternatively, the technique for calculating the gravitational field without calculating the gravitational potential was proposed in the book [16], but the final expression for the cylinder field is given in [16] without derivation. Following technique [16], we calculated the field and arrived at expressions (74, 79). Our expressions do not coincide with those given in [16–18]. Both the derivations and final results are presented in this article. Following the derivations in the articles [17, 18], we are going to find out analytically the reason of the discrepancies between different expressions and publish it elsewhere.

The article is arranged as follows. Standard deviation and shift are obtained in the next section. Section II is devoted to the AI phase and phase derivatives calculations, PDD and error budget for the scheme chosen in the article [1] are considered in the Sec. III. In the Sec. IV, it is shown that for the same total weight of the source mass, dividing it into 3 equal parts allows one to find a scheme in which all atomic variables become extreme,

and the calculation of the PDD and error budget for this scheme are carried out. In the Sec. V, a calculation was made for a 13-ton source mass. The conclusions are given in Sec. VI. Details of the numerical calculations and a derivation of the formula for the gravitational field of the cylinder are presented in the section Methods.

## I. SD AND SHIFT.

Let us consider the variation of the double difference (2)

$$\begin{aligned} \delta\Delta^{(2)}\phi & [\delta\mathbf{x}_{1C}, \delta\mathbf{v}_{1C}, \delta\mathbf{x}_{2C}, \delta\mathbf{v}_{2C}; \delta\mathbf{x}_{1F}, \delta\mathbf{v}_{1F}, \delta\mathbf{x}_{2F}, \delta\mathbf{v}_{2F}] \\ & = \delta\phi^{(C)} [\delta\mathbf{x}_{1C}, \delta\mathbf{v}_{1C}] - \delta\phi^{(C)} [\delta\mathbf{x}_{2C}, \delta\mathbf{v}_{2C}] \\ & - [\delta\phi^{(F)} (\delta\mathbf{x}_{1F}, \delta\mathbf{v}_{1F}) - \delta\phi^{(F)} (\delta\mathbf{x}_{2F}, \delta\mathbf{v}_{2F})], \end{aligned} \quad (6)$$

where  $\{\delta\mathbf{x}_{jI}, \delta\mathbf{v}_{jI}\}$  is the uncertainty of the launching position and velocity of the cloud  $j$  ( $j = 1$  or  $2$ ) for the source mass configuration  $I$  ( $I = C$  or  $F$ ),  $\delta\phi^{(I)} (\delta\mathbf{x}_{jI}, \delta\mathbf{v}_{jI})$  is the variation of the AI  $j$  phase, produced when the source mass gravity field is in the  $I$ -configuration. For the shift  $s$  and standard deviation  $\sigma$  defined as

$$\begin{aligned} s(\Delta^{(2)}\phi) &= \\ \left\langle \delta\Delta^{(2)}\phi [\delta\mathbf{x}_{1C}, \delta\mathbf{v}_{1C}, \delta\mathbf{x}_{2C}, \delta\mathbf{v}_{2C}; \delta\mathbf{x}_{1F}, \delta\mathbf{v}_{1F}, \delta\mathbf{x}_{2F}, \delta\mathbf{v}_{2F}] \right\rangle, \end{aligned} \quad (7a)$$

$$\sigma(\Delta_s^{(2)}\phi) = \left\{ \left\langle [\delta\Delta^{(2)}\phi (\delta\mathbf{x}_{1C}, \delta\mathbf{v}_{1C}, \delta\mathbf{x}_{2C}, \delta\mathbf{v}_{2C}; \delta\mathbf{x}_{1F}, \delta\mathbf{v}_{1F}; \delta\mathbf{x}_{2F}, \delta\mathbf{v}_{2F})]^2 \right\rangle - s^2 (\Delta^{(2)}\phi) \right\}^{1/2} \quad (7b)$$

one finds

$$\begin{aligned} s(\Delta^{(2)}\phi) &= s[\phi^{(C)} (\delta\mathbf{x}_{1C}, \delta\mathbf{v}_{1C})] - s[\phi^{(C)} (\delta\mathbf{x}_{2C}, \delta\mathbf{v}_{2C})] \\ &- s[\phi^{(F)} (\delta\mathbf{x}_{1F}, \delta\mathbf{v}_{1F})] + s[\phi^{(F)} (\delta\mathbf{x}_{2F}, \delta\mathbf{v}_{2F})], \end{aligned} \quad (8a)$$

$$\sigma(\Delta^{(2)}\phi) = \left\{ \sum_{I=C,F} \sum_{j=1,2} \sigma^2 [\phi^{(I)} (\delta\mathbf{x}_{jI}, \delta\mathbf{v}_{jI})] \right\}^{1/2}, \quad (8b)$$

$$s[\phi^{(I)} (\delta\mathbf{x}_{jI}, \delta\mathbf{v}_{jI})] = \left\langle \delta\phi^{(I)} (\delta\mathbf{x}_{jI}, \delta\mathbf{v}_{jI}) \right\rangle, \quad (8c)$$

$$\begin{aligned} \sigma[\phi^{(I)} (\delta\mathbf{x}_{jI}, \delta\mathbf{v}_{jI})] &= \left\{ \left\langle [\delta\phi^{(I)} (\delta\mathbf{x}_{jI}, \delta\mathbf{v}_{jI})]^2 \right\rangle \right. \\ &\left. - \left\langle \delta\phi^{(I)} (\delta\mathbf{x}_{jI}, \delta\mathbf{v}_{jI}) \right\rangle^2 \right\}^{1/2} \end{aligned} \quad (8d)$$

One sees that the problem is reduced to the calculation of the shift  $s$  and SD  $\sigma$  of a variation  $\delta\phi[\delta\mathbf{x}, \delta\mathbf{v}]$ . The phase of the given AI at the given configuration of the source mass comprises two parts

$$\phi(\mathbf{x}, \mathbf{v}) = \phi_E(\mathbf{x}, \mathbf{v}) + \phi_s(\mathbf{x}, \mathbf{v}), \quad (9)$$

where for the phase induced by the Earth's field, under some simplifying assumptions (see, for example, [20]), one gets

$$\begin{aligned} \phi_E^{(I)}(\mathbf{x}_j, \mathbf{v}_j) &= \mathbf{k} \cdot \mathbf{g} T^2 + \mathbf{k} \cdot \Gamma_E T^2 (\mathbf{x} + \mathbf{v} T) \\ &+ \mathbf{k} \cdot \Gamma_E \mathbf{g} T^2 \left( \frac{7}{12} T^2 + T T_1 + \frac{1}{2} T_1^2 \right) \end{aligned} \quad (10)$$

where  $T_1$  is the time delay between the moment the atoms are launched and the 1st Raman pulse. For the vertical wave vector  $\mathbf{k} = (0, 0, k)$ , expanding Eq. (9) to the second order terms one gets

$$\begin{aligned} \delta\phi(\delta\mathbf{x}, \delta\mathbf{v}) &= \left( \tilde{\gamma}_{xm} + \frac{\partial\phi_s}{\partial x_m} \right) \delta x_m + \left( \tilde{\gamma}_{vm} + \frac{\partial\phi_s}{\partial v_m} \right) \delta v_m \\ &+ \frac{1}{2} \frac{\partial^2\phi_s}{\partial x_m \partial x_n} \delta x_m \delta x_n + \frac{1}{2} \frac{\partial^2\phi_s}{\partial v_m \partial v_n} \delta v_m \delta v_n \\ &+ \frac{\partial^2\phi_s}{\partial x_m \partial v_n} \delta x_m \delta v_n, \end{aligned} \quad (11)$$

where

$$\tilde{\gamma}_{xm} = k \Gamma_{E3m} T^2; \quad (12a)$$

$$\tilde{\gamma}_{vm} = T \tilde{\gamma}_{xm} \quad (12b)$$

A summation convention implicit in Eq. (11) will be used in all subsequent equations. Repeated indices and symbols appearing on the right-hand-side (rhs) of an equation are to be summed over, unless they also appear on the left-hand-side (lhs) of that equation. Let assume that the distribution functions of the uncertainties are sufficiently symmetric, and all odd moments are equal 0. The moments of the second and fourth orders are given by

$$\langle \delta q_m \delta q_n \rangle = \delta_{mn} \sigma^2(q_m), \quad (13a)$$

$$\begin{aligned} \langle \delta q_m \delta q_n \delta q_{m'} \delta q_{n'} \rangle &= \delta_{mn} \delta_{m'n'} \sigma^2(q_m) \sigma^2(q_{m'}) \\ &+ (\delta_{mm'} \delta_{nn'} + \delta_{mn'} \delta_{nm'}) \sigma^2(q_m) \sigma^2(q_n) \\ &+ \delta_{mn} \delta_{mm'} \delta_{mn'} \kappa(q_m) \sigma^4(q_m), \end{aligned} \quad (13b)$$

where  $q_i$  is either a position  $x_i$  or a velocity  $v_i$ ,  $\sigma(q_i)$  is SD of the uncertainty  $\delta q_i$ ,  $\delta_{mn}$  is Kronecker symbol,  $\kappa(q_m)$  is a cumulant of the given uncertainty  $\delta q_m$ , defined as

$$\kappa(q_m) = \frac{\langle \delta q_m^4 \rangle}{\sigma^4(q_m)} - 3. \quad (14)$$

Using the moments (13) one arrives at the following expressions for the SD and shift

$$\begin{aligned} \sigma[\phi(\delta\mathbf{x}, \delta\mathbf{v})] &= \left\{ \left( \tilde{\gamma}_{xm} + \frac{\partial\phi_s}{\partial x_m} \right)^2 \sigma^2(x_m) \right. \\ &\quad + \left( \tilde{\gamma}_{vm} + \frac{\partial\phi_s}{\partial v_m} \right)^2 \sigma^2(v_m) \\ &\quad + \frac{1}{2} \left[ \left( \frac{\partial^2\phi}{\partial x_m \partial x_n} \right)^2 \sigma^2(x_m) \sigma^2(x_n) \right. \\ &\quad \left. \left. + \left( \frac{\partial^2\phi}{\partial v_m \partial v_n} \right)^2 \sigma^2(v_m) \sigma^2(v_n) \right] \right. \\ &\quad + \left( \frac{\partial^2\phi}{\partial x_m \partial v_n} \right)^2 \sigma^2(x_m) \sigma^2(v_n) \\ &\quad \left. + \frac{1}{4} \left[ \left( \frac{\partial^2\phi}{\partial x_m^2} \right)^2 \kappa(x_m) \sigma^4(x_m) \right. \right. \\ &\quad \left. \left. + \left( \frac{\partial^2\phi}{\partial v_m^2} \right)^2 \kappa(v_m) \sigma^4(v_m) \right] \right\}^{1/2}, \quad (15a) \end{aligned}$$

$$s[\phi(\delta\mathbf{x}, \delta\mathbf{v})] = \frac{1}{2} \left( \frac{\partial^2\phi}{\partial x_m^2} \sigma^2(x_m) + \frac{\partial^2\phi}{\partial v_m^2} \sigma^2(v_m) \right), \quad (15b)$$

One sees that, even for the symmetric uncertainties distribution, the knowledge of the uncertainties' SDs is not sufficient. One has to know also uncertainties' cumulants (14). The exclusion here is Gaussian distributions, for which the cumulants

$$\kappa(x_m) = \kappa(v_m) = 0. \quad (16)$$

Further calculations will be performed only for these distributions.

For the each case considered below we are going to calculate the double difference (2) and relative contributions to the SD (15a) and shift (15b) from the each of two atom clouds at the each of two source mass configurations.

## II. THE PHASE AND PHASE DERIVATIVES OF THE ATOM INTERFEROMETER

To calculate the phase  $\phi_s^{(I)}$  produced by the gravitational field of the source mass, we use the results obtained in the article [21]. It is necessary to distinguish three contributions to the phase, classical, quantum, and Q-term (see Eqs. (62c, 64, 60c), (62d, 71, 60c), (89) in [21] for these three terms). For Q-term an estimate was obtained

$$\frac{\phi_Q}{\phi_s^{(I)}} \sim \frac{1}{24} \left( \frac{\hbar k T}{L M_a} \right)^2, \quad (17)$$

where  $M_a$  is the atom mass,  $L$  is the characteristic distance over which the gravitational potential of the test mass changes. For  $^{87}\text{Rb}$ , at  $L > 0.3\text{m}$ , the relative weight

of the Q-term does not exceed 2ppb, and we neglect it. For the remaining terms and the vertical effective wave vector,  $\mathbf{k} = \{0, 0, k\}$ , one gets

$$\phi_s^{(I)}(\mathbf{x}, \mathbf{v}) = k \int_0^T dt [(T-t) \delta g_3(\mathbf{a}(T+t)) + t \delta g_3(\mathbf{a}(t))], \quad (18)$$

where

$$\mathbf{a}(t) = \mathbf{x} + \mathbf{v}(T_1 + t) + \frac{1}{2} \mathbf{g} (T_1 + t)^2 + \mathbf{v}_r t, \quad (19)$$

the recoil velocity is given by

$$\mathbf{v}_r = \hbar \mathbf{k} / 2M_a, \quad (20)$$

$\delta g_3(\mathbf{x})$  is the vertical component of the gravitational field of the source mass. The derivatives of this phase of the first and second order are given by

$$\begin{aligned} \frac{\partial \phi_s^{(I)}(\mathbf{x}, \mathbf{v})}{\partial x_m} &= k \int_0^T dt [(T-t) \Gamma_{s3m}(\mathbf{a}(T+t)) \\ &\quad + t \Gamma_{s3m}(\mathbf{a}(t))], \quad (21a) \end{aligned}$$

$$\begin{aligned} \frac{\partial \phi_s^{(I)}(\mathbf{x}, \mathbf{v})}{\partial v_m} &= k \int_0^T dt [(T-t)(T_1 + T + t) \\ &\quad \times \Gamma_{s3m}(\mathbf{a}(T+t)) + t(T_1 + t) \Gamma_{s3m}(\mathbf{a}(t))], \quad (21b) \end{aligned}$$

$$\begin{aligned} \frac{\partial^2 \phi_s^{(I)}(\mathbf{x}, \mathbf{v})}{\partial x_m \partial x_n} &= k \int_0^T dt [(T-t) \chi_{s3mn}(\mathbf{a}(T+t)) \\ &\quad + t \chi_{s3mn}(\mathbf{a}(t))], \quad (21c) \end{aligned}$$

$$\begin{aligned} \frac{\partial^2 \phi_s^{(I)}(\mathbf{x}, \mathbf{v})}{\partial x_m \partial v_n} &= k \int_0^T dt [(T-t)(T_1 + T + t) \\ &\quad \times \chi_{s3mn}(\mathbf{a}(T+t)) + t(T_1 + t) \chi_{s3mn}(\mathbf{a}(t))], \quad (21d) \end{aligned}$$

$$\begin{aligned} \frac{\partial^2 \phi_s^{(I)}(\mathbf{x}, \mathbf{v})}{\partial v_m \partial v_n} &= k \int_0^T dt \left[ (T-t)(T_1 + T + t)^2 \right. \\ &\quad \left. \times \chi_{s3mn}(\mathbf{a}(T+t)) + t(T_1 + t)^2 \chi_{s3mn}(\mathbf{a}(t)) \right], \quad (21e) \end{aligned}$$

where  $\Gamma_{s3m}(\mathbf{x}) = \frac{\partial \delta g_3(\mathbf{x})}{\partial x_m}$  is the  $3m$ -component of the gravity-gradient tensor of the source mass field, and

$$\chi_{s3mn}(\mathbf{x}) = \frac{\partial^2 \delta g_3(\mathbf{x})}{\partial x_m \partial x_n} \quad (22)$$

is the  $3mn$ -component of the curvature tensor of this field.

## III. SOURCE MASS CONSISTING OF 2 HALVES.

We applied the formula for the cylinder field (74) to calculate the phases produced by different sets of cylinders. In this section, we consider the field geometry chosen in the article [1], see Fig. 1.

Two halves of the source mass, each including 12 tungsten alloy cylinders, move in a vertical direction from

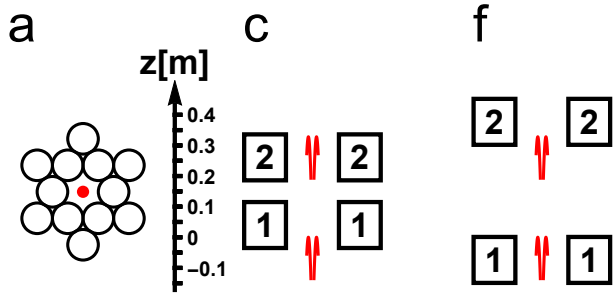


FIG. 1: The mutual positioning of the source mass halves 1 and 2, and atomic clouds. Top view (a), cross-sections  $x=0$  for  $C$ -configuration (c) and  $F$ -configuration (f). Trajectories of atoms are shown in red.

$C$ -configuration to  $F$ -configuration, in each of which one measures the phase difference of the first order (1), and then PDD (2). The following system parameters are important for calculation: cylinder density  $\rho = 18263 \text{ kg/m}^3$ , cylinder radius and height  $R = 0.0495 \text{ m}$  and  $h = 0.15011 \text{ m}$ , Newtonian gravitational constant  $G = 6.67408 \cdot 10^{-11} \text{ kg}^{-1} \text{ m}^3 \text{ s}^{-2}$  [22], the Earth's gravitational field  $g = 9.80492 \text{ m/s}^2$  [23], the delay between impulses  $T = 160 \text{ ms}$ , the time  $T_1 = 0$ , the effective wave vector  $k = 1.61058 \cdot 10^7 \text{ m}^{-1}$ , the mass of the  $^{87}\text{Rb}$   $M_a = 86.9092 \text{ a.u.}$  [24], atomic velocity at the moment of the first impulse action  $v = 1.62762 \text{ m/s}$  [25]. With respect to the apogee of the atomic trajectory in the lower interferometer, the  $z$ -coordinates of the centers of the halves of the source mass are equal to  $0.04 \text{ m}$  and  $0.261 \text{ m}$  in the  $C$ -configuration and  $-0.074 \text{ m}$  and  $0.377 \text{ m}$  in the  $F$ -configuration,  $z$ -coordinate of the atomic trajectory apogee in the upper interferometer is equal to  $0.328 \text{ m}$  (see Fig. 1c,f). Using Eq. (18) we got for PDD

$$\Delta^{(2)}\phi = 0.530535 \text{ rad}, \quad (23)$$

which is less than the value obtained in the article [1], by 3.2%. The difference seems to be related to the fact that in our calculations, the contributions from platforms and other sources of gravity were not taken into account. Details of the calculations of the error budget one can find in Methods Sec. VII A. For SDs achieved in [1]

$$\sigma(x_{jI}) = \sigma(y_{jI}) = 10^{-3} \text{ m}, \quad (24a)$$

$$\sigma(z_{jI}) = 10^{-4} \text{ m}, \quad (24b)$$

$$\sigma(v_{xjI}) = \sigma(v_{yjI}) = 6 \cdot 10^{-3} \text{ m/s}, \quad (24c)$$

$$\sigma(v_{zjI}) = 3 \cdot 10^{-3} \text{ m/s}, \quad (24d)$$

using Eqs. (49) one arrives to the RSD and the shift

$$\sigma(\delta\Delta_s^{(2)}\phi) = 275 \text{ ppm} [1 + 6.14 \cdot 10^{13} (\Gamma_{E31}^2 + \Gamma_{E32}^2)]^{1/2}, \quad (25a)$$

$$s(\delta\Delta_s^{(2)}\phi) = 199 \text{ ppm}. \quad (25b)$$

The non-diagonal matrix elements of the gradient tensor of the Earth's field consist of three contributions arising

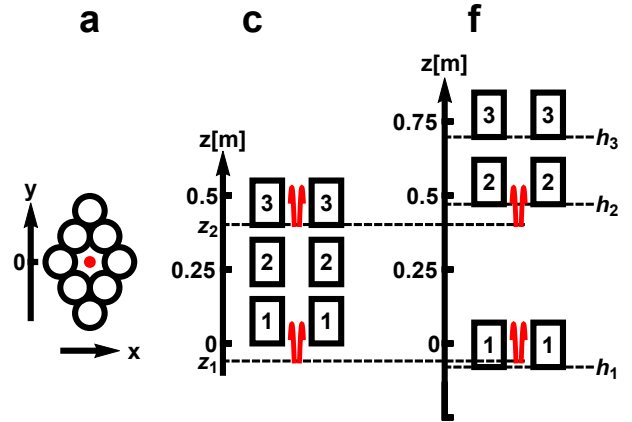


FIG. 2: The same as Fig. 1 but for the source mass conciting of 3 parts.

from the fact that the Geoid is not spherical, from the rotation of the Earth, and from the anomalous part of the field. The first two contributions were taken into account exactly [27], and they are 3 orders of magnitude smaller than the diagonal element  $\Gamma_{E33}$ . We failed to find any information about the anomalous part of the Earth's gravitational field. However, it is seen that the non-diagonal elements of the tensor can be neglected with an accuracy of not more than 10% if

$$\sqrt{\Gamma_{E31}^2 + \Gamma_{E32}^2} < 58.5E. \quad (26)$$

#### IV. SOURCE MASS CONSISTING OF 3 PARTS.

In this paper, we propose to divide the source mass not into two halves (as in the article [1]), but into 3 parts. The calculation showed that even in this case, 24 cylinders are enough for the gradient of the source mass gravitational field to compensate the gradient of the Earth's field. A symmetrical in the horizontal plane configuration of the source mass is shown in Fig. 2.

In a  $C$ -configuration, according to [4] and unlike [1] we have chosen for calculations in this section the distance between the lower and upper set of cylinders  $dh = 0.05 \text{ m}$ . One could use the local maximum and minimum of the phase (9) in the coordinate and velocity space

$$z_1 = -0.059 \text{ m}, z_2 = 0.402 \text{ m}, v_{z1} = v_{z2} = v = 1.563 \text{ m/s}, \quad (27)$$

from which atomic clouds of the 1st and 2nd AI should be launched. The phases of the interferometers (18) will be equal

$$\left\{ \phi_s^{(C)}(z_1, v), \phi_s^{(C)}(z_2, v) \right\} = \{0.144896 \text{ rad}, -0.150477 \text{ rad}\}. \quad (28)$$

The launching velocity in (27) is close to the velocity of the atomic fountain [28]  $gT$ , differing from it only in the third digit,

$$\delta v = v - gT \approx -6 \cdot 10^{-3} \text{ m/s} \quad (29)$$

This difference, however, is sufficient to exclude the parasitic signal [29], which occurs when atoms interact with a Raman pulse having an opposite sign of the effective wave vector. Indeed, the Raman frequency detuning for the parasitic signal  $\delta = 2k\delta v \approx -2 \cdot 10^5 \text{ s}^{-1}$ . If the duration of the  $\pi$ -pulse  $\tau \sim 60 \mu\text{s}$ , then the absolute value of the detuning  $\delta$  is an order of magnitude greater than the inverse pulse duration, and the probability of excitation of atoms by a parasitic Raman field is negligible, is estimated to be about 4%.

Let us now consider the  $F$ -configuration, see Fig. 2f. We are looking for an arrangement of parts of the source mass where the points (27) are still extremes, i.e. the coordinates of the parts of the source mass  $\{h_1, h_2, h_3\}$  are the roots of a system of 4 equations (4) with a constraint (3). There can be at least 2 such solutions. We have found and offer it for use a numerical solution

$$\{h_1, h_2, h_3\} = \{-0.080\text{m}, 0.470\text{m}, 0.697\text{m}\}, \quad (30)$$

when the point  $\{z_1, v\}$  becomes the local minimum, and the point  $\{z_2, v\}$  becomes the local maximum of the AI phase,

$$\left\{ \phi_s^{(F)}(z_1, v), \phi_s^{(F)}(z_2, v) \right\} = \{-0.065578\text{rad}, 0.107647\text{rad}\} \quad (31)$$

Using Eqs. (1, 2, 28, 31) one gets for PDD

$$\Delta^{(2)}\phi = 0.468599\text{rad}. \quad (32)$$

Details of the calculations of the error budget one can find in Methods Sec. VII B. For SDs (24) achieved in [1] using Eqs. (50) one arrives to the RSD and the shift

$$\sigma \left( \delta \Delta^{(2)}\phi \right) = 75\text{ppm} \left[ 1 + 1.05 \cdot 10^{15} (\Gamma_{E31}^2 + \Gamma_{E32}^2) \right]^{1/2}, \quad (33a)$$

$$s \left( \delta \Delta^{(2)}\phi \right) = 120\text{ppm}. \quad (33b)$$

The non-diagonal elements of the gravity-gradient tensor of the Earth field,  $\Gamma_{E31}$  and  $\Gamma_{E32}$ , can be neglected with an accuracy of not more than 10% if

$$\sqrt{\Gamma_{E31}^2 + \Gamma_{E32}^2} < 6.5E. \quad (34)$$

## V. 13-TON SOURCE MASS

We have already mentioned above that G. Rosi proposed and studied [2] a new approach to the measurement of  $G$  with an accuracy of 10 ppm, based on the technique of eliminating the gravity-gradient terms [14]. In addition to the new technique, estimates have been performed for the source mass weight increased to the 13 tons, time separation between Raman pulses increased to

$$T = 243\text{ms}, \quad (35)$$

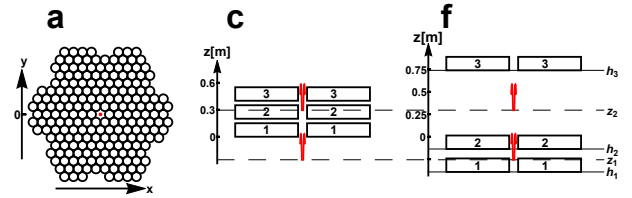


FIG. 3: The same as Fig. 2 but for the 13-ton source mass.

and the uncertainty of the velocity of atomic clouds reduced to

$$\sigma(v_{xjI}) = \sigma(v_{yjI}) = 2\text{mm/s}, \quad (36a)$$

$$\sigma(v_{zjI}) = 0.3\text{mm/s}. \quad (36b)$$

In this section, we tested our method of dividing the source mass into 3 parts for parameters close to those proposed in [2] and for the source mass consisting of cylinders used in [1]. We chose the location of the cylinders on 3 floors shown in Fig. 3. It is easy to see that the cylinders are still positioned symmetrically in the horizontal plane, and their total weight only slightly succeeds 13 tons. This arrangement of the cylinders is a natural generalization of the geometry chosen in the [1].

In a  $C$ -configuration, one could use the local maximum and minimum of the phase (9) in the coordinate and velocity space

$$z_1 = -0.257\text{m}, z_2 = 0.296\text{m}, v_{z1} = v_{z2} = v = 2.377\text{m/s}, \quad (37)$$

from which it is necessary to launch atomic clouds of the 1st and 2nd AI. The phases of the interferometers (18) will be equal

$$\left\{ \phi_s^{(C)}(z_1, v), \phi_s^{(C)}(z_2, v) \right\} = \{1.61114\text{rad}, -1.53727\text{rad}\}. \quad (38)$$

Let us now consider the  $F$ -configuration, see Fig. 2f. We are looking for an arrangement of parts of the source mass where the points (27) are still extremes, i.e. the coordinates of the parts of the source mass  $\{h_1, h_2, h_3\}$  are the roots of a system of 4 equations (4) with a constraint (3). There can be at least 2 such solutions. We have found and offer it for use a numerical solution

$$\{h_1, h_2, h_3\} = \{-0.377\text{m}, -0.153\text{m}, 0.561\text{m}\}, \quad (39)$$

when the point  $\{z_1, v\}$  becomes the local minimum, and the point  $\{z_2, v\}$  becomes the local maximum of the AI phase,

$$\left\{ \phi_s^{(F)}(z_1, v), \phi_s^{(F)}(z_2, v) \right\} = \{-0.724302\text{rad}, -0.015028\text{rad}\} \quad (40)$$

Using Eqs. (1, 2, 28, 31) one gets for PDD

$$\Delta^{(2)}\phi = 3.85769\text{rad}. \quad (41)$$

Details of the calculations of the error budget one can find in Methods Sec. VII C. For SDs (24a, 24b, 36) using

Eqs. (51) one arrives to the RSD and the shift

$$\sigma(\delta\Delta^{(2)}\phi) = 23\text{ppm} [1 + 5.84 \cdot 10^{14} (\Gamma_{E31}^2 + \Gamma_{E32}^2)]^{1/2}, \quad (42\text{a})$$

$$s(\delta\Delta^{(2)}\phi) = 45\text{ppm}. \quad (42\text{b})$$

The non-diagonal elements of the gravity-gradient tensor of the Earth field,  $\Gamma_{E31}$  and  $\Gamma_{E32}$ , can be neglected with an accuracy of not more than 10% if

$$\sqrt{\Gamma_{E31}^2 + \Gamma_{E32}^2} < 19E. \quad (43)$$

## VI. CONCLUSION

This article is devoted to the calculation of the error budget in the measurement of the Newtonian gravitational constant  $G$  by atomic interferometry methods. Using the technique [16], we obtained expressions for the gravitational field of the cylinder, which is used in these measurements.

Despite the compensation of the gradient of the Earth gravitational field at the points of apogees of the atomic trajectories achieved in the article [1], an absence of this compensation along the entire trajectory leads to the influence of the Earth's field on the  $G$  measurement accuracy. To overcome this influence, we propose to use source mass divided on 3 or more parts

The main attention in this article is paid to the calculation of standard deviation (SD) and the shift of the PDD due to the uncertainties of the mean values of the initial coordinates and the velocities of atomic clouds  $\{\delta\mathbf{x}, \delta\mathbf{v}\}$ . We propose to include in the error budget new terms. They are originated from the quadratic dependence of the variation of the AI phases on  $\{\delta\mathbf{x}, \delta\mathbf{v}\}$ . The shift arises only after including those terms. At the conditions realized in the article [1], calculations brings us to the shift (25b) and to the opposite relative correction  $\Delta G/G = -199\text{ppm}$ , which is larger than corrections considered in [1]. After including this correction, the value of the gravitational constant  $G$  should be shifted to

$$G = 6.67058\text{m}^3\text{kg}^{-1}\text{s}^{-2} \quad (44)$$

from the value  $G = 6.67191\text{m}^3\text{kg}^{-1}\text{s}^{-2}$  measured in [1]. Monte Carlo simulation was used in [3] to determine the constant  $G$ . In principle, if one includes in the simulation the variations in the spatial centers of atomic clouds and the centers of the atomic velocity distribution, the shift (25b) would be included in the averaging over random samples of the atomic coordinates and velocities. However, these variations, according to [3], were not included in the Monte Carlo simulation, which allows us to suggest shifting the measurement result of the constant  $G$  to the value (44).

Another discrepancy with article [3] is the measurement accuracy. According to our calculation for the

atomic coordinates' and velocities' SDs (24), which were achieved in [1], the measurement accuracy of  $G$  should not be less than 275ppm, see Eq. (25a), while according to [1] the total accuracy was 148ppm.

We propose to generalize the method [4] as follows. In the  $C$ -configuration, when all the parts of the source mass are pieced together, we look for local extremes of the total phase of the atomic interferometer (9), using the Eqs. (10, 18-20). In addition to the atomic coordinates, which were varied in [4], we vary also the atomic velocities. Calculations have shown that the atomic velocities at the points of local maximum and minimum coincide. The task now is to ensure that these found points remain extreme in the  $F$ -configuration. At the same time, in order for the contribution to the PDD from the  $F$ -configuration to be positive, the former maximum point  $(z_1, v_{z1})$  must become the minimum point, and the former minimum point  $(z_2, v_{z2})$  must become the maximum point. The necessary condition for this is that the phase of the atomic interferometer, as a function of the positions of the source mass parts, must satisfy a system of 4 equations (4) with a restraint (3), i.e., at least, the phase must be a function of 3 parameters of the source mass. In contrast to [1, 4], we propose to divide it into 3 parts, and to choose for the parameters the 3 vertical coordinates of the source mass parts  $\{h_1, h_2, h_3\}$ .

We considered this procedure in Section IV for the same number of cylinders as in [1, 4]. **In fact, it is shown that a simple redistribution of the cylinders between the floors of the source mass should lead to an improvement in the accuracy of the Newton gravitational constant measurement by a factor of 3.7 [compare Eqs. (25a, 33a)].**

Following the statement [2], that 13-ton source mass can be implemented in the experiment, we increased the number of cylinders to 606 (more than 25 times). At the same time, the PDD increased only 8.4 times [compare Eqs. (41) and (32)], and this increase is partly due to an increase in the delay time between the Raman pulses  $T$ . This example shows that an increase in the weight of the source mass does not even lead to a proportional signal increase. More promising here is an increase in the signal due to the larger value of the effective wave vector  $k$ , longer interrogation time  $T$ , and the optimal aspect ratio of the source mass. Due to these factors we predicted [6] PDD  $\Delta_s^{(2)}\phi = 386.527\text{rad}$  even for a source mass  $M = 1080\text{kg}$ .

We showed that for the parameters chosen for estimates in [2], our methods of dividing a source mass in 3 parts, leads to the measurement accuracy 23ppm, comparable with 10ppm accuracy predicted in [2] for an alternative method [14] of eliminating the gravity gradient tensor.

We also performed calculations for the source mass consisting of 4 quarters. In this case, in the  $F$ -configuration, the 1st and 2nd floors of the source mass can be located under the 1st AI, while the 3rd and 4th floors above the 2nd AI. As a result, the con-

tribution to the PDD from the point of the minimum ( $z_1, v_{z1}$ ), or from the point of the maximum ( $z_2, v_{z2}$ ) will increase leading possibly to the smaller value of RSD. If one still uses 24 cylinders, as in [1, 4], after dividing them in 4 equal quarters, the gravitational field is too weak to compensate the gradient of the Earth's field. As a result, there are no local extremes in the  $F$ -configuration. To get extremes one needs at least 32 cylinders. It is reasonable for us to consider this situation, since even larger amount of cylinders have been used, for example, in the article [30]. We arrived to the following result (see Methods Sec. VII D 1 )

$$\Delta^2\phi = 0.523494 \text{ rad}, \quad (45a)$$

$$\sigma(\delta\Delta^{(2)}\phi) = 60 \text{ ppm} [1 + 1.32 \cdot 10^{-15} (\Gamma_{E31}^2 + \Gamma_{E32}^2)]^{1/2}, \quad (45b)$$

$$s(\delta\Delta^{(2)}\phi) = 96 \text{ ppm}. \quad (45c)$$

Since we had to change the weight of the source mass, comparison with the results (32, 33) is unfair.

We also considered the case of 4 quarters for 13-ton source mass (see Methods Sec. VII D 2 ), and arrived to the following result

$$\Delta^2\phi = 4.72602 \text{ rad}, \quad (46a)$$

$$\sigma(\delta\Delta_s^{(2)}\phi) = 17 \text{ ppm} [1 + 6.54 \cdot 10^{14} (\Gamma_{E31}^2 + \Gamma_{E32}^2)]^{1/2}, \quad (46b)$$

$$s(\delta\Delta_s^{(2)}\phi) = 35 \text{ ppm}. \quad (46c)$$

Comparing this with Eqs. (41, 42) shows that using a source mass consisting of 4 quarters could increase PDD in a factor 1.22 and improve the measurement accuracy in a factor 1.35.

Another application of our formulas is the calculation of the systematic error due to the finite size of atomic

clouds and their finite temperature [6, 11]. Let us now assume that  $\delta\mathbf{x}$  is the deviation of the atom from the center of the cloud and  $\delta\mathbf{v}$  is the deviation from the center of the atomic velocity distribution. If the temperatures are small enough to ignore the Doppler frequency shift, and the aperture of the optical field is large enough to assume that the areas of the Raman pulses do not depend on the position of atoms in the cloud, then the only reason for the dependence of the PDD on  $\{\delta\mathbf{x}, \delta\mathbf{v}\}$  is that the gravitational field  $\delta\mathbf{g}[\mathbf{x}(t)]$  is not the same for different atoms in the cloud. Averaging the phase of the AI over an atomic distribution one will receive from the equation (11)

$$\langle\delta\phi\rangle = \frac{1}{4} \left( a_m^2 \frac{\partial^2\phi}{\partial x_m^2} + v_{0m}^2 \frac{\partial^2\phi}{\partial v_m^2} \right), \quad (47)$$

where  $a_m = \sqrt{2\langle\delta x_m^2\rangle}$  and  $v_{0m} = \sqrt{2\langle\delta v_m^2\rangle}$  are the radius and thermal velocity of the atomic cloud along the  $m$ -axis. Here we pay attention to the fact that at equal radii,  $a_x = a_y = a_z$ , and temperatures,  $v_{0x} = v_{0y} = v_{0z}$ , the systematic error (47) disappears. This follows from the Eqs. (21c, 21e) and from the fact that the gravitational field obeys the Laplace equation and, therefore, the trace of the gravitational field curvature tensor (22)

$$\sum_{m=1}^3 \chi_{s3mm} = 0.$$

## Acknowledgments

Author is appreciated to Dr. M. Prevedeli for the fruitful discussions and to Dr. G. Rosi for the explanation of some points in the article [2].

---

[1] G. Rosi, F. Sorrentino, L. Cacciapuoti, M. Prevedeli & G. M. Tino, Precision measurement of the Newtonian gravitational constant using cold atoms, *Nature* **510**, 518 (2014).

[2] G. Rosi, A proposed atom interferometry determination of G at  $10^{-5}$  using a cold atomic fountain, *Metrologia* **55**, 50 (2018).

[3] B. Ya. Dubetskii, A. P. Kazantsev, V. P. Chebotayev, V. P. Yakovlev, Interference of atoms and formation of atomic spatial arrays in light fields, *Pis'ma Zh. Eksp. Teor. Fiz.* **39**, 531 (1984) [*JETP Lett.* **39**, 649 (1984)].

[4] G. Lamporesi, Determination of the gravitational constant by atom interferometry, Thesis, University of Florence, 2006.

[5] J. B. Fixler, G. T. Foster, J. M. McGuirk, M. A. Kasevich, Atom Interferometer Measurement of the Newtonian Constant of Gravity, *Science* **315**, 74 (2007).

[6] B. Dubetsky, Atom interferometers' phases at the presence of heavy masses; their use to measure Newtonian gravitational constant; optimization, error model, perspectives, In Proceedings of the MPLP-2016 Conference, Novosibirsk, Russia, 2016, IOP Conf. Series: Journal of Physics: Conf. Series **793** 012006 (2017).

[7] S. M. Dickerson, J. M. Hogan, A. Sugarbaker, D. M. S. Johnson, M. A. Kasevich, Multi-axis inertial sensing with long-time point source atom interferometry, *Phys. Rev. Lett.* **111**, 083001 (2013).

[8] T. Kovachy, J. M. Hogan, A. Sugarbaker, S. M. Dickerson, C. A. Donnelly, C. Overstreet, and M. A. Kasevich, Matter Wave Lensing to Picokelvin Temperatures, *Phys. Rev. Lett.* **114** 143004 (2015).

[9] T. Kovachy, P. Asenbaum, C. Overstreet, C. A. Donnelly, S. M. Dickerson, A. Sugarbaker, J. M. Hogan & M. A. Kasevich, Quantum superposition at the half-metre scale, *Nature* **528**, 530 (2015).

[10] G. W. Biedermann, X. Wu, L. Deslauriers, S. Roy, C.

Mahadeswaraswamy, M. A. Kasevich, Testing Gravity with Cold-Atom Interferometers, *Phys. Rev. A* **91**, 033629 (2015).

[11] B. Dubetsky, Optimization and error model for atom interferometry technique to measure Newtonian gravitational constant, arXiv:1407.7287v2 [physics.atom-ph].

[12] M. J. Snadden, J. M. McGuirk, P. Bouyer, K. G. Haritos, and M. A. Kasevich, Measurement of the Earth's Gravity Gradient with an Atom Interferometer-Based Gravity Gradiometer, *Phys. Rev. Lett.* **81**, 971 (1998).

[13] A. Peters, K. Y. Chung, and S. Chu, Measurement of gravitational acceleration by dropping atoms, *Nature*, **400**, 849 (1999).

[14] A. Roura, Circumventing Heisenberg's uncertainty principle in atom interferometry tests of the equivalence principle, *Phys. Rev. Lett.* **118**, 160401 (2017).

[15] Z. F. Seidov, P. I. Skvirsky, Gravitational potential and energy of homogeneous rectangular parallelepiped, arXiv:astro-ph/0002496v1.

[16] Y. T. Chen, A. Cook, Gravitational experiment in the laboratory, Cambridge University Press, Cambridge 1993.

[17] M. N. Nabighian, The Gravitational attraction of a right vertical circular cylinder at points external to it, *Geofis. Pura e Appl.* **53**, 45 (1962).

[18] D. Miles, Closed-form expressions for the non-axial component of the gravitational field of an arbitrary cylinder segment, *Journal of Applied Geophysics* **159**, 621 (2018).

[19] A. M. Mathai, S. B. Provost, Quadratic forms in random variables: theory and applications, Marcel Dekker, INC, New York, 1993.

[20] B. Dubetsky, Full elimination of the gravity-gradient terms in atom interferometry, *Appl. Phys. B* **125**, 187 (2019).

[21] B. Dubetsky, S. B. Libby and P. Berman, Atom interferometry in the presence of an external test mass, *Atoms*, **4**, 14 (2016).

[22] P. J. Mohr, D. B. Newell, B. N. Taylor, CODATA Recommended Values of the Fundamental Physical Constants: 2014, *Rev. Mod. Phys.*, **88**, 035009 (2016).

[23] M. de Angelis, F. Greco, A. Pistorio, N. Poli, M. Prevedelli, G. Saccorotti, F. Sorrentino, and G. M. Tino, Measurement of absolute gravity acceleration in Firenze, *Solid Earth Discuss.* **3**, 43 (2011).

[24] M. P. Bradley, J. V. Porto, S. Rainville, J. K. Thompson, and D. E. Pritchard, Penning Trap Measurements of the Masses of  $^{133}\text{Cs}$ ,  $^{87,85}\text{Rb}$ , and  $^{23}\text{Na}$  with Uncertainties  $<0.2$  ppb, *Phys. Rev. Lett.* **83**, 4510 (1999).

[25] This velocity is equal to  $v = gT_a$ , where  $T_a$  is a time between the 1st pulse and the moment when the atoms reach the apogee of their trajectory. According to the data in the successive arXiv copy [26] of the article [1],  $T_a = 166\text{ms}$ , while from the article [1] itself, one arrives to another value  $T_a = 154\text{Ms}$ . The value  $T_a = 166\text{ms}$  is chosen here.

[26] G. Rosi, F. Sorrentino, L. Cacciapuoti, M. Prevedelli & G. M. Tino, Precision measurement of the Newtonian gravitational constant using cold atoms, arXiv:1412.7954 [physics.atom-ph].

[27] M. A. Kasevich and B. Dubetsky, Kinematic Sensors Employing Atom Interferometer Phases, US Patent 7,317,184 (2005).

[28] R. G. Beausoleil, T. W. Hansch, Ultra-high resolution two-photon optical Ramsey spectroscopy of an atomic fountain, *Phys. Rev. A* **33**, 1661 (1986).

[29] I. Perrin, J. Bernard, Y. Bidel, N. Zahzam, C. Blanchard, and A. Bresson, Zero-velocity atom interferometry using a retroreflected frequency chirped laser, arXiv:1907.04403 [physics.atom-ph]

[30] G. Rosi, L. Cacciapuoti, F. Sorrentino, M. Menchetti, M. Prevedelli, G. M. Tino, Measurement of the Gravity-Field Curvature by Atom Interferometry, *Phys. Rev. Lett.* **114**, 013001 (2015).

## VII. METHODS

### A. Source mass consisting of 2 halves.

For the source mass and atomic fountains positioning shown in the Fig. 1, the Table I contains relative contributions to the PDD from two configurations. Besides the phase values, linear and quadratic terms in the relative phase variations, due to the uncertainties of atomic coordinates and velocities, obtained using Eqs. (11, 12, 21), are also given. Here and below we used the value of the  $zz$ -component of the gravity gradient tensor of the Earth field,

$$\Gamma_{E33} = 3.11 \cdot 10^{-6} s^{-2}, \quad (48)$$

measured in the article [1]. Using data from the Table I and Eqs. (8a, 8b, 15, 16), we obtained following error budget and shift

$$\begin{aligned} \sigma\left(\Delta_s^{(2)}\phi\right) = & \{0.104\sigma^2(z_{1C}) + 0.0137\sigma^2(z_{2C}) + 1.42 \cdot 10^{-3}\sigma^2(v_{z1C}) + 2.24 \cdot 10^{-4}\sigma^2(v_{z2C}) \\ & + 0.0173\sigma^2(z_{1F}) + 0.269\sigma^2(z_{2F}) + 1.75 \cdot 10^{-4}\sigma^2(v_{z1F}) + 4.66 \cdot 10^{-3}\sigma^2(v_{z2F}) \\ & + \sum_{j=1,2} \sum_{I=C,F} [6.04 \cdot 10^{11} (\Gamma_{E31}^2 \sigma^2(x_{jI}) + \Gamma_{E32}^2 \sigma^2(y_{jI})) + 1.55 \cdot 10^{10} (\Gamma_{E31}^2 \sigma^2(v_{xjI}) + \Gamma_{E32}^2 \sigma^2(v_{yjI}))] \\ & + 305 [\sigma^4(x_{1C}) + \sigma^4(y_{1C})] + 1220\sigma^4(z_{1C}) + 296 [\sigma^4(x_{2C}) + \sigma^4(y_{2C})] + 1180\sigma^4(z_{2C}) \\ & + 0.282 [\sigma^4(v_{x1C}) + \sigma^4(v_{y1C})] + 1.13\sigma^4(v_{z1C}) + 0.247 [\sigma^4(v_{x2C}) + \sigma^4(v_{y2C})] + 0.987\sigma^4(v_{z2C}) \\ & + 15.9 [\sigma^2(x_{1C}) \sigma^2(v_{x1C}) + \sigma^2(y_{1C}) \sigma^2(v_{y1C})] + 63.5\sigma^2(z_{1C}) \sigma^2(v_{z1C}) \\ & + 16.4 [\sigma^2(x_{2C}) \sigma^2(v_{x2C}) + \sigma^2(y_{2C}) \sigma^2(v_{y2C})] + 65.6\sigma^2(z_{2C}) \sigma^2(v_{z2C}) \\ & + 478 [\sigma^4(x_{1F}) + \sigma^4(y_{1F})] + 1910\sigma^4(z_{1F}) + 490 [\sigma^4(x_{2F}) + \sigma^4(y_{2F})] + 1960\sigma^4(z_{2F}) + \\ & + 0.406 [\sigma^4(v_{x1F}) + \sigma^4(v_{y1F})] + 1.63\sigma^4(v_{z1F}) + 0.439 [\sigma^4(v_{x2F}) + \sigma^4(v_{y2F})] + 1.76\sigma^4(v_{z2F}) \\ & + 26.0 [\sigma^2(x_{1F}) \sigma^2(v_{x1F}) + \sigma^2(y_{1F}) \sigma^2(v_{y1F})] + 104\sigma^2(z_{1F}) \sigma^2(v_{z1F}) \\ & + 25.8 [\sigma^2(x_{2F}) \sigma^2(v_{x2F}) + \sigma^2(y_{2F}) \sigma^2(v_{y2F})] + 103\sigma^2(z_{2F}) \sigma^2(v_{z2F})\}^{1/2}, \end{aligned} \quad (49a)$$

$$\begin{aligned} s\left(\Delta_s^{(2)}\phi\right) = & 12.3 [\sigma^2(x_{1C}) + \sigma^2(y_{1C})] - 24.7\sigma^2(z_{1C}) + 12.2 [\sigma^2(x_{2C}) + \sigma^2(y_{2C})] - 24.3\sigma^2(v_{z2C}) \\ & + 0.375 [\sigma^2(v_{x1C}) + \sigma^2(v_{y1C})] - 0.750\sigma^2(v_{z1C}) + 0.351 [\sigma^2(v_{x2C}) + \sigma^2(v_{y2C})] - 0.702\sigma^2(v_{z2C}) \\ & + 15.5 [\sigma^2(x_{1F}) + \sigma^2(y_{1F})] - 30.9\sigma^2(z_{1F}) + 15.7 [\sigma^2(x_{2F}) + \sigma^2(y_{2F})] - 31.3\sigma^2(z_{2F}) \\ & + 0.451 [\sigma^2(v_{x1F}) + \sigma^2(v_{y1F})] - 0.902\sigma^2(v_{z1F}) + 0.468 [\sigma^2(v_{x2F}) + \sigma^2(v_{y2F})] - 0.937\sigma^2(v_{z2F}). \end{aligned} \quad (49b)$$

### B. Source mass consisting of 3 parts.

For the source mass and atomic fountains positioning shown in the Fig. 2, using Eq. (48) we arrived to the relative contributions to the PDD listed in the Table II. One sees that despite the choice of extreme points, linear dependences on  $\{\delta z_{jI}, \delta v_{zjI}\}$  in the phase variation do not completely disappear. This is because extrema (27) and positions of the source mass parts in the  $F$ -configuration (30) were found approximately. Here and below negligible linear terms will be excluded from the calculation. Using data from this table and Eqs. (8a, 8b, 15, 16), we obtained following error

budget and shift

$$\begin{aligned} \sigma \left( \Delta_s^{(2)} \phi \right) = & \left\{ 10^{10} \sum_{j=1,2} \sum_{I=C,F} [77.4 (\Gamma_{E31}^2 \sigma^2 (x_{jI}) + \Gamma_{E32}^2 \sigma^2 (y_{jI})) + 1.98 (\Gamma_{E31}^2 \sigma^2 (v_{xjI}) + \Gamma_{E32}^2 \sigma^2 (v_{yjI}))] \right. \\ & + 22.5 \sigma^4 (x_{1C}) + 77.4 \sigma^4 (y_{1C}) + 183 \sigma^4 (z_{1C}) + 49.9 \sigma^4 (x_{2C}) + 130 \sigma^4 (y_{2C}) + 341 \sigma^4 (z_{2C}) + \\ & + 0.0316 \sigma^4 (v_{x1C}) + 0.0926 \sigma^4 (v_{y1C}) + 0.232 \sigma^4 (v_{z1C}) + 0.0275 \sigma^4 (v_{x2C}) + 0.0825 \sigma^4 (v_{y2C}) + 0.205 \sigma^4 (v_{z2C}) \\ & + 1.15 \sigma^2 (x_{1C}) \sigma^2 (v_{x1C}) + 3.96 \sigma^2 (y_{1C}) \sigma^2 (v_{y1C}) + 9.39 \sigma^2 (z_{1C}) \sigma^2 (v_{z1C}) \\ & + 2.56 \sigma^2 (x_{2C}) \sigma^2 (v_{x2C}) + 6.66 \sigma^2 (y_{2C}) \sigma^2 (v_{y2C}) + 17.5 \sigma^2 (z_{2C}) \sigma^2 (v_{z2C}) + \\ & + 352 \sigma^4 (x_{1F}) + 525 \sigma^4 (y_{1F}) + 1740 \sigma^4 (z_{1F}) + 78.3 \sigma^4 (x_{2F}) + 1685 \sigma^4 (y_{2F}) + 475 \sigma^4 (z_{2F}) \\ & + 0.262 \sigma^4 (v_{x1F}) + 0.392 \sigma^4 (v_{y1F}) + 1.30 \sigma^4 (v_{z1F}) + 0.0858 \sigma^4 (v_{x2F}) + 0.177 \sigma^4 (v_{y2F}) + 0.509 \sigma^4 (v_{z2F}) \\ & + 18.0 \sigma^2 (x_{1F}) \sigma^2 (v_{x1F}) + 26.9 \sigma^2 (y_{1F}) \sigma^2 (v_{y1F}) + 88.9 \sigma^2 (z_{1F}) \sigma^2 (v_{z1F}) \\ & \left. + 4.01 \sigma^2 (x_{2F}) \sigma^2 (v_{x2F}) + 8.58 \sigma^2 (y_{2F}) \sigma^2 (v_{y2F}) + 24.3 \sigma^2 (z_{2F}) \sigma^2 (v_{z2F}) \right\}^{1/2} \end{aligned} \quad (50a)$$

$$\begin{aligned} s \left( \Delta_s^{(2)} \phi \right) = & 3.36 \sigma^2 (x_{1C}) + 6.22 \sigma^2 (y_{1C}) - 9.58 \sigma^2 (z_{1C}) + 5.00 \sigma^2 (x_{2C}) + 8.07 \sigma^2 (y_{2C}) - 13.1 \sigma^2 (z_{2C}) \\ & + 0.126 \sigma^2 (v_{x1C}) + 0.215 \sigma^2 (v_{y1C}) - 0.341 \sigma^2 (v_{z1C}) + 0.117 \sigma^2 (v_{x2C}) + 0.203 \sigma^2 (v_{y2C}) - 0.320 \sigma^2 (v_{z2C}) \\ & + 13.3 \sigma^2 (x_{1F}) + 16.2 \sigma^2 (y_{1F}) - 29.5 \sigma^2 (z_{1F}) + 6.26 \sigma^2 (x_{2F}) + 9.15 \sigma^2 (y_{2F}) - 15.4 \sigma^2 (z_{2F}) \\ & + 0.362 \sigma^2 (v_{x1F}) + 0.443 \sigma^2 (v_{y1F}) - 0.805 \sigma^2 (v_{z1F}) + 0.207 \sigma^2 (v_{x2F}) + 0.297 \sigma^2 (v_{y2F}) - 0.504 \sigma^2 (v_{z2F}). \end{aligned} \quad (50b)$$

### C. 13-ton source mass.

For the source mass and atomic fountains positioning shown in the Fig. 3, using Eq. (48) we arrived to the relative contributions to the PDD listed in the Table III. Using data from this table and Eqs. (8a, 8b, 15, 16), we obtained following error budget and shift

$$\begin{aligned} \sigma \left( \Delta_s^{(2)} \phi \right) = & \left\{ 10^9 \sum_{j=1,2} \sum_{I=C,F} [60.8 (\Gamma_{E31}^2 \sigma^2 (x_{jI}) + \Gamma_{E32}^2 \sigma^2 (y_{jI})) + 3.59 (\Gamma_{E31}^2 \sigma^2 (v_{xjI}) + \Gamma_{E32}^2 \sigma^2 (v_{yjI}))] \right. \\ & + 42.4 \sigma^4 (x_{1C}) + 42.6 \sigma^4 (y_{1C}) + 170 \sigma^4 (z_{1C}) + 36.9 \sigma^4 (x_{2C}) + 37.0 \sigma^4 (y_{2C}) + 148 \sigma^4 (z_{2C}) + \\ & + 0.176 \sigma^4 (v_{x1C}) + 0.177 \sigma^4 (v_{y1C}) + 0.706 \sigma^4 (v_{z1C}) + 0.146 [\sigma^4 (v_{x2C}) + \sigma^4 (v_{y2C})] + 0.583 \sigma^4 (v_{z2C}) \\ & + 5.01 \sigma^2 (x_{1C}) \sigma^2 (v_{x1C}) + 5.03 \sigma^2 (y_{1C}) \sigma^2 (v_{y1C}) + 20.1 \sigma^2 (z_{1C}) \sigma^2 (v_{z1C}) \\ & + 4.36 \sigma^2 (x_{2C}) \sigma^2 (v_{x2C}) + 4.37 \sigma^2 (y_{2C}) \sigma^2 (v_{y2C}) + 17.4 \sigma^2 (z_{2C}) \sigma^2 (v_{z2C}) + \\ & + 35.9 [\sigma^4 (x_{1F}) + \sigma^4 (y_{1F})] + 144 \sigma^4 (z_{1F}) + 52.1 \sigma^4 (x_{2F}) + 52.0 \sigma^4 (y_{2F}) + 208 \sigma^4 (z_{2F}) \\ & + 0.139 [\sigma^4 (v_{x1F}) + \sigma^4 (v_{y1F})] + 0.556 \sigma^4 (v_{z1F}) + 0.213 \sigma^4 (v_{x2F}) + 0.212 \sigma^4 (v_{y2F}) + 0.850 \sigma^4 (v_{z2F}) \\ & + 4.24 [\sigma^2 (x_{1F}) \sigma^2 (v_{x1F}) + \sigma^2 (y_{1F}) \sigma^2 (v_{y1F})] + 17.0 \sigma^2 (z_{1F}) \sigma^2 (v_{z1F}) \\ & \left. + 6.15 [\sigma^2 (x_{2F}) \sigma^2 (v_{x2F}) + \sigma^2 (y_{2F}) \sigma^2 (v_{y2F})] + 24.6 \sigma^2 (z_{2F}) \sigma^2 (v_{z2F}) \right\}^{1/2}, \end{aligned} \quad (51a)$$

$$\begin{aligned} s \left( \Delta_s^{(2)} \phi \right) = & 4.61 [\sigma^2 (x_{1C}) + \sigma^2 (y_{1C})] - 9.22 \sigma^2 (z_{1C}) + 4.29 \sigma^2 (x_{2C}) + 4.30 \sigma^2 (y_{2C}) - 8.59 \sigma^2 (z_{2C}) \\ & + 0.297 [\sigma^2 (v_{x1C}) + \sigma^2 (v_{y1C})] - 0.594 \sigma^2 (v_{z1C}) + 0.270 [\sigma^2 (v_{x2C}) + \sigma^2 (v_{y2C})] - 0.540 \sigma^2 (v_{z2C}) \\ & + 4.24 [\sigma^2 (x_{1F}) + \sigma^2 (y_{1F})] - 8.47 \sigma^2 (z_{1F}) + 5.10 [\sigma^2 (x_{2F}) + \sigma^2 (y_{2F})] - 10.2 \sigma^2 (z_{2F}) \\ & + 0.264 [\sigma^2 (v_{x1F}) + \sigma^2 (v_{y1F})] - 0.527 \sigma^2 (v_{z1F}) + 0.326 [\sigma^2 (v_{x2F}) + \sigma^2 (v_{y2F})] - 0.652 \sigma^2 (v_{z2F}). \end{aligned} \quad (51b)$$

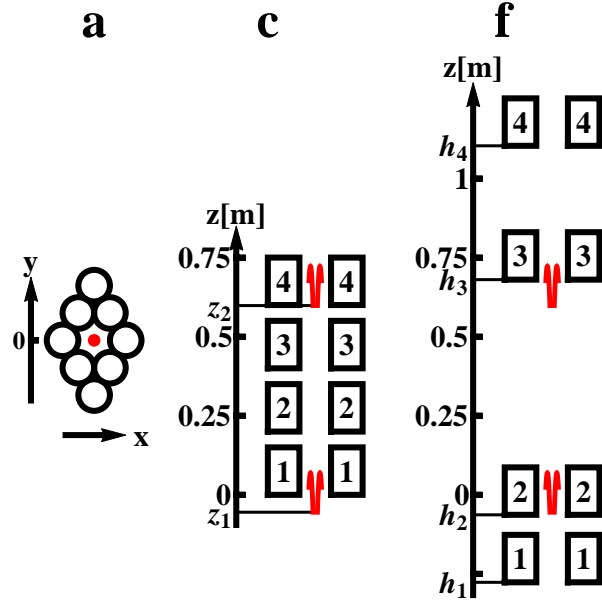


FIG. 4: The same as Fig. 2 but for the source mass consisting of 4 quarters.

#### D. Source mass consisting of 4 quarters

##### 1. Minimal source mass

We performed calculations for the source mass geometry shown in Fig. 4.

This is a minimal amount of cylinders used in [1], when 4 quarters of the source mass produce a sufficiently strong gravitational field to make all atomic variables extreme in the both configurations. Instead of Eqs. (27, 28, 30-32) we arrived to the following results

$$z_1 = -0.0550\text{m}, z_2 = 0.599\text{m}, v_{z1} = v_{z2} = v = 1.563\text{m/s}, \quad (52\text{a})$$

$$\left\{ \phi_s^{(C)}(z_1, v), \phi_s^{(C)}(z_2, v) \right\} = \{0.150754\text{rad}, -0.157906\text{rad}\}, \quad (52\text{b})$$

$$\{h_1, h_2, h_3, h_4\} = \{-0.277\text{m}, -0.0632\text{m}, 0.681\text{m}, 1.10\text{m}\}, \quad (52\text{c})$$

$$\left\{ \phi_s^{(F)}(z_1, v), \phi_s^{(F)}(z_2, v) \right\} = \{-0.118576\text{rad}, 0.096258\text{rad}\}, \quad (52\text{d})$$

$$\Delta^2 \phi = 0.523494\text{rad}. \quad (52\text{e})$$

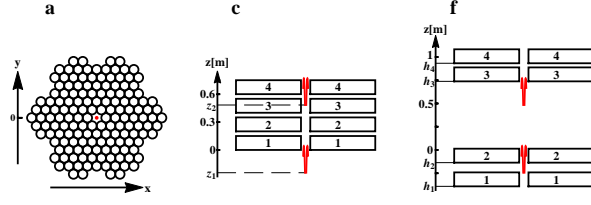


FIG. 5: The same as Fig. 3 but for the source mass consisting of 4 quarters.

Relative contributions to the PDD listed now in the Table IV. Using data from this table and Eqs. (8a, 8b, 15, 16), we obtained following error budget and shift

$$\begin{aligned} \sigma \left( \Delta_s^{(2)} \phi \right) = & \left\{ 10^{10} \sum_{j=1,2} \sum_{I=C,F} \left[ 62.0 (\Gamma_{E31}^2 \sigma^2 (x_{jI}) + \Gamma_{E32}^2 \sigma^2 (y_{jI})) + 1.59 (\Gamma_{E31}^2 \sigma^2 (v_{xjI}) + \Gamma_{E32}^2 \sigma^2 (v_{yjI})) \right] \right. \\ & + 9.16 \sigma^4 (x_{1C}) + 41.1 \sigma^4 (y_{1C}) + 89.1 \sigma^4 (z_{1C}) + 24.2 \sigma^4 (x_{2C}) + 74.8 \sigma^4 (y_{2C}) + 184 \sigma^4 (z_{2C}) \\ & + 0.0155 \sigma^4 (v_{x1C}) + 0.0534 \sigma^4 (v_{y1C}) + 0.126 \sigma^4 (v_{z1C}) + 0.0116 \sigma^4 (v_{x2C}) + 0.0449 \sigma^4 (v_{y2C}) + 0.102 \sigma^4 (v_{z2C}) \\ & + 0.469 \sigma^2 (x_{1C}) \sigma^2 (v_{x1C}) + 2.11 \sigma^2 (y_{1C}) \sigma^2 (v_{y1C}) + 4.56 \sigma^2 (z_{1C}) \sigma^2 (v_{z1C}) \\ & + 1.24 \sigma^2 (x_{2C}) \sigma^2 (v_{x2C}) + 3.83 \sigma^2 (y_{2C}) \sigma^2 (v_{y2C}) + 9.43 \sigma^2 (z_{2C}) \sigma^2 (v_{z2C}) \\ & + 98.9 \sigma^4 (x_{1F}) + 193 \sigma^4 (y_{1F}) + 569 \sigma^4 (z_{1F}) + 168 \sigma^4 (x_{2F}) + 282 \sigma^4 (y_{2F}) + 885 \sigma^4 (z_{2F}) + \\ & + 0.0643 \sigma^4 (v_{x1F}) + 0.132 \sigma^4 (v_{y1F}) + 0.381 \sigma^4 (v_{z1F}) + 0.157 \sigma^4 (v_{x2F}) + 0.265 \sigma^4 (v_{y2F}) + 0.830 \sigma^4 (v_{z2F}) \\ & + 5.06 \sigma^2 (x_{1F}) \sigma^2 (v_{x1F}) + 9.90 \sigma^2 (y_{1F}) \sigma^2 (v_{y1F}) + 29.1 \sigma^2 (z_{1F}) \sigma^2 (v_{z1F}) \\ & \left. + 8.60 \sigma^2 (x_{2F}) \sigma^2 (v_{x2F}) + 14.4 \sigma^2 (y_{2F}) \sigma^2 (v_{y2F}) + 45.3 \sigma^2 (z_{2F}) \sigma^2 (v_{z2F}) \right\}^{1/2}, \end{aligned} \quad (53a)$$

$$\begin{aligned} s \left( \Delta_s^{(2)} \phi \right) = & 2.14 \sigma^2 (x_{1C}) + 4.53 \sigma^2 (y_{1C}) - 6.67 \sigma^2 (z_{1C}) + 3.48 \sigma^2 (x_{2C}) + 6.12 \sigma^2 (y_{2C}) - 9.60 \sigma^2 (z_{2C}) \\ & + 0.0879 \sigma^2 (v_{x1C}) + 0.163 \sigma^2 (v_{y1C}) - 0.251 \sigma^2 (v_{z1C}) + 0.0762 \sigma^2 (v_{x2C}) + 0.150 \sigma^2 (v_{y2C}) - 0.226 \sigma^2 (v_{z2C}) \\ & + 7.03 \sigma^2 (x_{1F}) + 9.83 \sigma^2 (y_{1F}) - 16.9 \sigma^2 (z_{1F}) + 9.17 \sigma^2 (x_{2F}) + 11.9 \sigma^2 (y_{2F}) - 21.0 \sigma^2 (z_{2F}) \\ & + 0.179 \sigma^2 (v_{x1F}) + 0.257 \sigma^2 (v_{y1F}) - 0.437 \sigma^2 (v_{z1F}) + 0.281 \sigma^2 (v_{x2F}) + 0.364 \sigma^2 (v_{y2F}) - 0.644 \sigma^2 (v_{z2F}). \end{aligned} \quad (53b)$$

Substituting here uncertainties of the atomic variables (24) one gets instead of Eqs. (33, 34)

$$\sigma \left( \delta \Delta^{(2)} \phi \right) = 60 \text{ppm} [1 + 1.32 \cdot 10^{15} (\Gamma_{E31}^2 + \Gamma_{E32}^2)]^{1/2}, \quad (54a)$$

$$s \left( \delta \Delta^{(2)} \phi \right) = 96 \text{ppm}, \quad (54b)$$

$$\sqrt{\Gamma_{E31}^2 + \Gamma_{E32}^2} < 6E. \quad (54c)$$

## 2. 13-ton source mass

A symmetric in the horizontal plane source mass, which can be divided in 4 quarters and has a minimal total weight exceeding 13 tons, is shown in the fig. 5

Instead of Eqs. (37 - 41) we arrived to the following results

$$z_1 = -0.244 \text{m}, z_2 = 0.483 \text{m}, v_{z1} = v_{z2} = v = 2.377 \text{m/s}, \quad (55a)$$

$$\left\{ \phi_s^{(C)} (z_1, v), \phi_s^{(C)} (z_2, v) \right\} = \{1.73221 \text{rad}, -1.67974 \text{rad}\}, \quad (55b)$$

$$\{h_1, h_2, h_3, h_4\} = \{-0.391 \text{m}, -0.136 \text{m}, 0.738 \text{m}, 0.933 \text{m}\}, \quad (55c)$$

$$\left\{ \phi_s^{(F)} (z_1, v), \phi_s^{(F)} (z_2, v) \right\} = \{-0.58469 \text{rad}, 0.72938 \text{rad}\}, \quad (55d)$$

$$\Delta^2 \phi = 4.72602 \text{rad}. \quad (55e)$$

Relative contributions to the PDD listed now in the Table V. Using data from this table and Eqs. (8a, 8b, 15, 16), we obtained following error budget and shift

$$\begin{aligned} \sigma \left( \Delta_s^{(2)} \phi \right) = & \left\{ 10^9 \sum_{j=1,2} \sum_{I=C,F} [40.5 (\Gamma_{E31}^2 \sigma^2 (x_{jI}) + \Gamma_{E32}^2 \sigma^2 (y_{jI})) + 2.39 (\Gamma_{E31}^2 \sigma^2 (v_{xjI}) + \Gamma_{E32}^2 \sigma^2 (v_{yjI}))] \right. \\ & + 20.7 \sigma^4 (x_{1C}) + 20.6 \sigma^4 (y_{1C}) + 82.6 \sigma^4 (z_{1C}) + 26.3 \sigma^4 (x_{2C}) + 26.1 \sigma^4 (y_{2C}) + 105 \sigma^4 (z_{2C}) \\ & + 0.0896 \sigma^4 (v_{x1C}) + 0.0889 \sigma^4 (v_{y1C}) + 0.357 \sigma^4 (v_{z1C}) + 0.0998 \sigma^4 (v_{x2C}) + 0.0991 \sigma^4 (v_{y2C}) + 0.398 \sigma^4 (v_{z2C}) \\ & + 2.45 \sigma^2 (x_{1C}) \sigma^2 (v_{x1C}) + 2.43 \sigma^2 (y_{1C}) \sigma^2 (v_{y1C}) + 9.75 \sigma^2 (z_{1C}) \sigma^2 (v_{z1C}) \\ & + 3.10 \sigma^2 (x_{2C}) \sigma^2 (v_{x2C}) + 3.08 \sigma^2 (y_{2C}) \sigma^2 (v_{y2C}) + 12.4 \sigma^2 (z_{2C}) \sigma^2 (v_{z2C}) \\ & + 23.8 [\sigma^4 (x_{1F}) + \sigma^4 (y_{1F})] + 95.2 \sigma^4 (z_{1F}) + 28.9 [\sigma^4 (x_{2F}) + \sigma^4 (y_{2F})] + 116 \sigma^4 (z_{2F}) + \\ & + 0.0874 \sigma^4 (v_{x1F}) + 0.0872 \sigma^4 (v_{y1F}) + 0.349 \sigma^4 (v_{z1F}) + 0.121 [\sigma^4 (v_{x2F}) + \sigma^4 (v_{y2F})] + 0.485 \sigma^4 (v_{z2F}) \\ & + 2.81 [\sigma^2 (x_{1F}) \sigma^2 (v_{x1F}) + \sigma^2 (y_{1F}) \sigma^2 (v_{y1F})] + 11.2 \sigma^2 (z_{1F}) \sigma^2 (v_{z1F}) \\ & \left. + 3.42 \sigma^2 (x_{2F}) \sigma^2 (v_{x2F}) + 3.41 \sigma^2 (y_{2F}) \sigma^2 (v_{y2F}) + 13.7 \sigma^2 (z_{2F}) \sigma^2 (v_{z2F}) \right\}^{1/2}, \end{aligned} \quad (56a)$$

$$\begin{aligned} s \left( \Delta_s^{(2)} \phi \right) = & 3.22 \sigma^2 (x_{1C}) + 3.21 \sigma^2 (y_{1C}) - 6.43 \sigma^2 (z_{1C}) + 3.62 \sigma^2 (x_{2C}) + 3.61 \sigma^2 (y_{2C}) - 7.24 \sigma^2 (z_{2C}) \\ & + 0.212 \sigma^2 (v_{x1C}) + 0.211 \sigma^2 (v_{y1C}) - 0.423 \sigma^2 (v_{z1C}) + 0.223 [\sigma^2 (v_{x2C}) + \sigma^2 (v_{y2C})] - 0.446 \sigma^2 (v_{z2C}) \\ & + 3.45 [\sigma^2 (x_{1F}) + \sigma^2 (y_{1F})] - 6.90 \sigma^2 (z_{1F}) + 3.80 [\sigma^2 (x_{2F}) + \sigma^2 (y_{2F})] - 7.60 \sigma^2 (z_{2F}) \\ & + 0.209 [\sigma^2 (v_{x1F}) + \sigma^2 (v_{y1F})] - 0.418 \sigma^2 (v_{z1F}) + 0.246 [\sigma^2 (v_{x2F}) + \sigma^2 (v_{y2F})] - 0.492 \sigma^2 (v_{z2F}). \end{aligned} \quad (56b)$$

Substituting here uncertainties of the atomic variables (24a, 24b, 36) one gets instead of Eqs. (42, 43)

$$\sigma \left( \delta \Delta_s^{(2)} \phi \right) = 17 \text{ppm} [1 + 6.54 \cdot 10^{14} (\Gamma_{E31}^2 + \Gamma_{E32}^2)]^{1/2}, \quad (57a)$$

$$s \left( \delta \Delta_s^{(2)} \phi \right) = 35 \text{ppm}, \quad (57b)$$

$$\sqrt{\Gamma_{E31}^2 + \Gamma_{E32}^2} < 18E. \quad (57c)$$

### E. Gravity field of the homogeneous cylinder

#### 1. Axial component

It is convenient [16] to explore the following expression for the potential of the gravitational field of a homogeneous cylinder  $\Phi(\mathbf{x})$

$$\Phi(r, z) = -2G\rho \int_0^R dy \int_{r-\sqrt{R^2-y^2}}^{r+\sqrt{R^2-y^2}} d\xi \int_{z-h}^z \frac{d\zeta}{\sqrt{y^2 + \xi^2 + \zeta^2}}, \quad (58)$$

where  $\rho$ ,  $R$ , and  $h$  are the density, radius, and height of the cylinder,  $(r, z, \psi = 0)$  are the cylindrical coordinates of the vector  $\mathbf{x}$ . For an axial component of the gravitational field,  $\delta g_3(r, z) = -\partial_z \Phi(r, z)$ , one gets

$$\delta g_3(r, z) = 2G\rho g_3(r, \zeta)_{\zeta=z-h}^{\zeta=z}, \quad (59)$$

where the function

$$g_3(r, \zeta) = \int_0^R dy \int_{r-\sqrt{R^2-y^2}}^{r+\sqrt{R^2-y^2}} \frac{d\xi}{\sqrt{y^2 + \xi^2 + \zeta^2}} \quad (60)$$

can be represented as

$$\begin{aligned} g_3(r, \zeta) &= \int_0^R dy \ln \frac{t_+(y)}{t_-(y)} \\ &= - \int_0^R y \left( \frac{dt_+}{t_+} - \frac{dt_-}{t_-} \right), \end{aligned} \quad (61a)$$

$$t_{\pm}(y) = r \pm \sqrt{R^2 - y^2} + \left( \zeta^2 + r^2 + R^2 \pm 2r\sqrt{R^2 - y^2} \right)^{1/2} \quad (61b)$$

Since  $t_+(R) = t_-(R) \equiv t(R) \leq t_{\pm}(0)$  one can write

$$g_3(r, \zeta) = \int_{t(R)}^{t_+(0)} \frac{dt}{t} y_+(t) + \int_{t_-(0)}^{t(R)} \frac{dt}{t} y_-(t), \quad (62)$$

where  $y_{\pm}(t)$  is the root of the equation  $t_{\pm}(y) = t$ . To find this root, consider the functions  $x_{\pm}(t) = \sqrt{R^2 - y_{\pm}^2(t)}$ ,

$$0 < x_{\pm}(t) < R. \quad (63)$$

For them one gets

$$x_{\pm}(t) = \pm t + \sqrt{\zeta^2 + R^2 + 2tr} \text{ or } \pm t - \sqrt{\zeta^2 + R^2 + 2tr} \quad (64)$$

Since  $t + \sqrt{\zeta^2 + R^2 + 2tr} > R$ , then one should choose  $x_+(t) = t - \sqrt{\zeta^2 + R^2 + 2tr}$ . Since  $t_-(0) > r - R + |r - R| > 0$ ,  $t - \sqrt{\zeta^2 + R^2 + 2tr} < 0$ , hence  $x_-(t) = \sqrt{\zeta^2 + R^2 + 2tr} - t$  or

$$x_{\pm}(t) = \pm \left( t - \sqrt{\zeta^2 + R^2 + 2tr} \right). \quad (65)$$

Therefore, one concludes that the functions  $y_{\pm}(t)$  are coincident and equal to

$$y_+(t) = y_-(t) = y(t) = \left[ 2t \left( \sqrt{\zeta^2 + R^2 + 2tr} - r \right) - t^2 - \zeta^2 \right]^{1/2} \quad (66)$$

and.

$$g_3(r, \zeta) = \int_{t_-(0)}^{t_+(0)} \frac{dt}{t} y(t). \quad (67)$$

Introducing new variable,

$$u = \sqrt{\zeta^2 + R^2 + 2tr} - r, \quad (68)$$

for which

$$u[t_{\pm}(0)] \equiv u_{\pm} = \sqrt{\zeta^2 + (r \pm R)^2}, \quad (69a)$$

$$y(t) = \frac{\sqrt{q(u^2)}}{2r}, \quad (69b)$$

$$q(\eta) = \{u_+^2 - \eta\} \{\eta - u_-^2\}, \quad (69c)$$

$$dt = \frac{u+r}{r} du \quad (69d)$$

and so

$$g_3(r, \zeta) = I + I', \quad (70a)$$

$$I = \int_{u_-}^{u_+} \frac{du}{\sqrt{q(u^2)}} J(u), \quad (70b)$$

$$J(u) = \frac{q(u^2)(r^2 - \zeta^2 - R^2 - u^2)}{w(u^2)}, \quad (70c)$$

$$I' = \frac{1}{2r} \int_{u_-^2}^{u_+^2} d\eta J'(\eta), \quad (70d)$$

$$J'(\eta) = \frac{(\eta - \zeta^2 - R^2 - r^2)}{\sqrt{q(\eta)} w(\eta)}, \quad (70e)$$

$$w(\eta) = (\eta - \eta_1)(\eta - \eta_2), \quad (70f)$$

$$\eta_{1,2} = \left( r \pm \sqrt{\zeta^2 + R^2} \right)^2. \quad (70g)$$

Using equality

$$w(\eta) + q(\eta) = -4r^2\zeta^2, \quad (71)$$

one can show that the integrand  $J'(\eta)$  is an antisymmetric function with respect to the middle point  $\eta = \{u^2[t_+(0)] + u^2[t_-(0)]\}/2$ , and, therefore, the term (70d) is equal 0. At the same time, expanding  $J(u)$  into partial fractions, one obtains

$$g_3(r, \zeta) = (R^2 + \zeta^2 - r^2) I_1 + I_2 + I_{3+} + I_{3-}, \quad (72a)$$

$$I_1 = \int_{u_-}^{u_+} \frac{du}{\sqrt{q(u^2)}}, \quad (72b)$$

$$I_2 = \int_{u_-}^{u_+} \frac{du u^2}{\sqrt{q(u^2)}}, \quad (72c)$$

$$I_{3\pm} = 2r\zeta^2 \left( r \pm \sqrt{\zeta^2 + R^2} \right) \int_{u_-}^{u_+} \frac{du}{\sqrt{q(u^2)}(u^2 - \eta_{1,2})} \quad (72d)$$

The integrals (72), one can compute using the substitution

$$u = \sqrt{u_+^2 - (u_+^2 - u_-^2) \sin^2 \phi} \quad (73)$$

Finally, one arrives at the following expression for the axial component of the cylinder's field

$$\delta g_3(r, z) = 2G\rho g_3(r, \zeta) \Big|_{\zeta=z-h}^{\zeta=z}, \quad (74a)$$

$$\begin{aligned} g_3(r, \zeta) = & \frac{(\zeta^2 + R^2 - r^2)}{\sqrt{\zeta^2 + (r + R)^2}} K(k) + \sqrt{\zeta^2 + (r + R)^2} E(k) \\ & + \frac{\zeta^2}{\sqrt{\zeta^2 + (r + R)^2}} \sum_{j=\pm 1} \left[ \frac{r + j\sqrt{\zeta^2 + R^2}}{R - j\sqrt{\zeta^2 + R^2}} \Pi \left( \frac{2R}{R - j\sqrt{\zeta^2 + R^2}} | k \right) \right], \end{aligned} \quad (74b)$$

$$k = \sqrt{\frac{4rR}{\zeta^2 + (r + R)^2}}, \quad (74c)$$

where  $K(k)$ ,  $E(k)$  and  $\Pi(\alpha|k)$  are the complete elliptic integrals of the first, second and third order respectively.

## 2. Radial component

For the radial component of the gravitational field  $\delta g_r(r, z) = -\partial_r \Phi(r, z)$  one obtains from (58)

$$\delta g_r(r, z) = 2G\rho g_r(r, \zeta) \zeta^{\zeta=z}_{\zeta=z-h}, \quad (75a)$$

$$g_r(r, \zeta) = - \int_0^R y \left( \frac{dt_+}{t_+} - \frac{dt_-}{t_-} \right), \quad (75b)$$

$$t_{\pm}(y) = \zeta + \left[ \zeta^2 + r^2 + R^2 \pm 2r\sqrt{R^2 - y^2} \right]^{1/2} \quad (75c)$$

Since still  $t_+(R) = t_-(R) \leq t_{\pm}(0)$ , one gets,

$$g_r(r, \zeta) = \int_{t_-(0)}^{t(R)} \frac{dt}{t} y_-(t) + \int_{t(R)}^{t_+(0)} \frac{dt}{t} y_+(t), \quad (76)$$

where  $y_{\pm}(t)$  are functions inverse to (75c). Since these functions are the same

$$y_+(t) = y_-(t) \equiv y(t) = \frac{1}{2r} \left[ 4r^2 R^2 - (t^2 - 2\zeta t - r^2 - R^2)^2 \right]^{1/2}, \quad (77)$$

then, choosing as an integration variable  $u = t - \zeta$ , one finds that

$$g_r(r, \zeta) = I + I', \quad (78a)$$

$$I = -\frac{\zeta}{2r} \int_{u_-}^{u_+} \frac{du q(u^2)}{(u^2 - \zeta^2) \sqrt{q(u^2)}}, \quad (78b)$$

$$I' = \frac{1}{4r} \int_{u_-^2}^{u_+^2} \frac{d\eta \sqrt{q(\eta)}}{(\eta - \zeta^2)}, \quad (78c)$$

where  $u_{\pm}$  and  $q(\eta)$  are given by Eqs. (69a, 69c). Because  $u_{\pm}^2 - \zeta^2$  and  $q(\eta + \zeta^2)$  are independent of  $\zeta$ , the term  $I'$  gives no contribution to the acceleration (75a) and can be omitted. While using the substitution (73), one reduces the integral in (78b) to elliptic integrals, which brings us to the next final result

$$\delta g_r(r, z) = 2G\rho g_r(r, \zeta) \zeta^{\zeta=z}_{\zeta=z-h}, \quad (79a)$$

$$g_r(r, \zeta) = \frac{\zeta}{2r\sqrt{\zeta^2 + (r+R)^2}} \left[ -(\zeta^2 + 2r^2 + 2R^2) K(k) + (\zeta^2 + (r+R)^2) E(k) + \frac{(r^2 - R^2)^2}{(r+R)^2} \Pi \left( \frac{4rR}{(r+R)^2} | k \right) \right], \quad (79b)$$

where  $k$  is given by Eq. (74c).

---

[1] M. Prevedelli, L. Cacciapuoti, G. Rosi, F. Sorrentino and G. M. Tino, Measuring the Newtonian constant of gravitation  $G$  with an atomic interferometer, Phil. Trans. R. Soc. A **372**, 20140030 (2014)

TABLE I: Source mass consisting of 2 halves. Relative contributions to the phase double difference (PDD) and error budget for two configurations of source mass

Term	$C$ -configuration	$F$ -configuration
$\phi_s^I(z_i, v_{zi}) / \Delta^2 \phi$	0.354, -0.330	-0.143, 0.172
Linear in position	$0.322\delta z_{1C} + 0.117\delta z_{2C} + 7.77 \cdot 10^5$ $\times [\Gamma_{E31}(\delta x_{1C} - \delta x_{2C}) + \Gamma_{E32}(\delta y_{1C} - \delta y_{2C})]$	$0.132\delta z_{1F} + 0.518\delta z_{2F} - 7.77 \cdot 10^5$ $\times [\Gamma_{E31}(\delta x_{1F} - \delta x_{2F}) + \Gamma_{E32}(\delta y_{1F} - \delta y_{2F})]$
Linear in velocity	$0.0377\delta v_{z1C} + 0.0150\delta v_{z2C} + 1.24 \cdot 10^5$ $\times [\Gamma_{E31}(\delta v_{x1C} - \delta v_{x2C}) + \Gamma_{E32}(\delta v_{y1C} - \delta v_{y2C})]$	$0.0132\delta v_{z1F} + 0.0683\delta v_{z2F} - 1.24 \cdot 10^5$ $\times [\Gamma_{E31}(\delta v_{x1F} - \delta v_{x2F}) + \Gamma_{E32}(\delta v_{y1F} - \delta v_{y2F})]$
Nonlinear in position	$12.3(\delta x_{1C}^2 + \delta y_{1C}^2) - 24.7\delta z_{1C}^2$ $+ 12.2(\delta x_{2C}^2 + \delta y_{2C}^2) - 24.3\delta z_{2C}^2$	$15.5(\delta x_{1F}^2 + \delta y_{1F}^2) - 30.9\delta z_{1F}^2$ $+ 15.7(\delta x_{2F}^2 + \delta y_{2F}^2) - 31.3\delta z_{2F}^2$
Nonlinear in velocity	$0.375(\delta v_{x1C}^2 + \delta v_{y1C}^2) - 0.750\delta v_{z1C}^2$ $+ 0.351(\delta v_{x2C}^2 + \delta v_{y2C}^2) - 0.702\delta v_{z2C}^2$	$0.451(\delta v_{x1F}^2 + \delta v_{y1F}^2) - 0.901\delta v_{z1F}^2$ $+ 0.468(\delta v_{x2F}^2 + \delta v_{y2F}^2) - 0.937\delta v_{z2F}^2$
Position-velocity cross term	$3.99(\delta v_{x1C}\delta x_{1C} + \delta v_{y1C}\delta y_{1C}) - 7.97\delta v_{z1C}\delta z_{1C}$ $+ 4.05(\delta v_{x2C}\delta x_{2C} + \delta v_{y2C}\delta y_{2C}) - 8.10\delta v_{z2C}\delta z_{2C}$	$5.10(\delta v_{x1F}\delta x_{1F} + \delta v_{y1F}\delta y_{1F}) - 10.2\delta v_{z1F}\delta z_{1F}$ $+ 5.08(\delta v_{x2F}\delta x_{2F} + \delta v_{y2F}\delta y_{2F}) - 10.2\delta v_{z2F}\delta z_{2F}$

TABLE II: The same as in Table I but for the source mass consisting of 3 parts

Term	$C$ -configuration	$F$ -configuration
$\phi_s^I(z_i, v_{zi}) / \Delta^2 \phi$	0.309, -0.321	-0.140, 0.230
Linear in position	$10^{-7}(-1.52\delta z_{1C} + 1.28\delta z_{2C}) + 8.80 \cdot 10^5$ $\times [\Gamma_{E31}(\delta x_{1C} - \delta x_{2C}) + \Gamma_{E32}(\delta y_{1C} - \delta y_{2C})]$	$10^{-8}(1.29\delta z_{1F} + 3.57\delta z_{2F}) - 8.80 \cdot 10^5$ $\times [\Gamma_{E31}(\delta x_{1F} - \delta x_{2F}) + \Gamma_{E32}(\delta y_{1F} - \delta y_{2F})]$
Linear in velocity	$10^{-8}(-3.38\delta v_{z1C} + 2.18\delta v_{z2C}) + 1.41 \cdot 10^5$ $\times [\Gamma_{E31}(\delta v_{x1C} - \delta v_{x2C}) + \Gamma_{E32}(\delta v_{y1C} - \delta v_{y2C})]$	$10^{-9}(-2.97\delta v_{z1F} - 5.26\delta v_{z2F}) - 1.41 \cdot 10^5$ $\times [\Gamma_{E31}(\delta v_{x1F} - \delta v_{x2F}) + \Gamma_{E32}(\delta v_{y1F} - \delta v_{y2F})]$
Nonlinear in position	$3.36\delta x_{1C}^2 + 6.22\delta y_{1C}^2 - 9.58\delta z_{1C}^2$ $+ 5.00\delta x_{2C}^2 + 8.07\delta y_{2C}^2 - 13.1\delta z_{2C}^2$	$13.3\delta x_{1F}^2 + 16.2\delta y_{1F}^2 - 29.5\delta z_{1F}^2$ $+ 6.26\delta x_{2F}^2 + 9.15\delta y_{2F}^2 - 15.4\delta z_{2F}^2$
Nonlinear in velocity	$0.126\delta v_{x1C}^2 + 0.215\delta v_{y1C}^2 - 0.341\delta v_{z1C}^2$ $+ 0.117\delta v_{x2C}^2 + 0.203\delta v_{y2C}^2 - 0.320\delta v_{z2C}^2$	$0.362\delta v_{x1F}^2 + 0.443\delta v_{y1F}^2 - 0.805\delta v_{z1F}^2$ $+ 0.207\delta v_{x2F}^2 + 0.297\delta v_{y2F}^2 - 0.504319\delta v_{z2F}^2$
Position-velocity cross term	$1.07\delta v_{x1C}\delta x_{1C} + 1.99\delta v_{y1C}\delta y_{1C} - 3.06\delta v_{z1C}\delta z_{1C}$ $+ 1.60\delta v_{x2C}\delta x_{2C} + 2.58\delta v_{y2C}\delta y_{2C} - 4.18\delta v_{z2C}\delta z_{2C}$	$4.24\delta v_{x1F}\delta x_{1F} + 5.19\delta v_{y1F}\delta y_{1F} - 9.43\delta v_{z1F}\delta z_{1F}$ $+ 2.00\delta v_{x2F}\delta x_{2F} + 2.93\delta v_{y2F}\delta y_{2F} - 4.93\delta v_{z2F}\delta z_{2F}$

TABLE III: The same as in Table I but for the 13 tons source mass.

Term	$C$ -configuration	$F$ -configuration
$\phi_s^I(z_i, v_{zi}) / \Delta^2 \phi$	0.418, -0.398	$-0.188, -3.90 \cdot 10^{-3}$
Linear in position	$10^{-10}(-11.0\delta z_{1C} + 8.63\delta z_{2C}) + 2.47 \cdot 10^5$ $\times [\Gamma_{E31}(\delta x_{1C} - \delta x_{2C}) + \Gamma_{E32}(\delta y_{1C} - \delta y_{2C})]$	$10^{-9}(-7.36\delta z_{1F} - 10.8\delta z_{2F}) - 2.47 \cdot 10^5$ $\times [\Gamma_{E31}(\delta x_{1F} - \delta x_{2F}) + \Gamma_{E32}(\delta y_{1F} - \delta y_{2F})]$
Linear in velocity	$10^{-10}(-2.97\delta v_{z1C} + 2.09\delta v_{z2C}) + 5.99 \cdot 10^4$ $\times [\Gamma_{E31}(\delta v_{x1C} - \delta v_{x2C}) + \Gamma_{E32}(\delta v_{y1C} - \delta v_{y2C})]$	$10^{-9}(-1.79\delta v_{z1F} - 2.25\delta v_{z2F}) - 5.99 \cdot 10^4$ $\times [\Gamma_{E31}(\delta v_{x1F} - \delta v_{x2F}) + \Gamma_{E32}(\delta v_{y1F} - \delta v_{y2F})]$
Nonlinear in position	$4.61(\delta x_{1C}^2 + \delta y_{1C}^2) - 9.22\delta z_{1C}^2$ $+ 4.29\delta x_{2C}^2 + 4.30\delta y_{2C}^2 - 8.59\delta z_{2C}^2$	$4.24[\delta x_{1F}^2 + \delta y_{1F}^2] - 8.47\delta z_{1F}^2$ $+ 5.10[\delta x_{2F}^2 + \delta y_{2F}^2] - 10.2\delta z_{2F}^2$
Nonlinear in velocity	$0.297(\delta v_{x1C}^2 + \delta v_{y1C}^2) - 0.594\delta v_{z1C}^2$ $+ 0.270(\delta v_{x2C}^2 + \delta v_{y2C}^2) - 0.540\delta v_{z2C}^2$	$0.264[\delta v_{x1F}^2 + \delta v_{y1F}^2] - 0.527\delta v_{z1F}^2$ $+ 0.326[\delta v_{x2F}^2 + \delta v_{y2F}^2] - 0.652\delta v_{z2F}^2$
Position-velocity cross term	$2.24(\delta v_{x1C}\delta x_{1C} + \delta v_{y1C}\delta y_{1C}) - 4.48\delta v_{z1C}\delta z_{1C}$ $+ 2.09(\delta v_{x2C}\delta x_{2C} + \delta v_{y2C}\delta y_{2C}) - 4.18\delta v_{z2C}\delta z_{2C}$	$2.06[\delta v_{x1F}\delta x_{1F} + \delta v_{y1F}\delta y_{1F}] - 4.12\delta v_{z1F}\delta z_{1F}$ $+ 2.48[\delta v_{x2F}\delta x_{2F} + \delta v_{y2F}\delta y_{2F}] - 4.96\delta v_{z2F}\delta z_{2F}$

TABLE IV: The same as in Table I but for the source mass geometry shown in Fig. 4.

Term	$C$ -configuration	$F$ -configuration
$\phi_s^T(z_i, v_{zi}) / \Delta^2 \phi$	0.288, -0.302	-0.227, 0.184
Linear in position	$10^{-8} (3.79 \delta z_{1C} - 139 \delta z_{2C}) + 7.88 \cdot 10^0 \times [\Gamma_{E31}(\delta x_{1C} - \delta x_{2C}) + \Gamma_{E32}(\delta y_{1C} - \delta y_{2C})]$	$10^{-7} (-2.45 \delta z_{1F} - 27.3 \delta z_{2F}) - 7.88 \cdot 10^0 \times [\Gamma_{E31}(\delta x_{1F} - \delta x_{2F}) + \Gamma_{E32}(\delta y_{1F} - \delta y_{2F})]$
Linear in velocity	$10^{-9} (6.92 \delta v_{z1C} - 296 \delta v_{z2C}) + 1.26 \cdot 10^5 \times [\Gamma_{E31}(\delta v_{x1C} - \delta v_{x2C}) + \Gamma_{E32}(\delta v_{y1C} - \delta v_{y2C})]$	$10^{-8} (-3.91 \delta v_{z1F} - 4.52 \delta v_{z2F}) - 1.26 \cdot 10^5 \times [\Gamma_{E31}(\delta v_{x1F} - \delta v_{x2F}) + \Gamma_{E32}(\delta v_{y1F} - \delta v_{y2F})]$
Nonlinear in position	$2.14 \delta x_{1C}^2 + 4.53 \delta y_{1C}^2 - 6.67 \delta z_{1C}^2 + 3.48 \delta x_{2C}^2 + 6.12 \delta y_{2C}^2 - 9.60 \delta z_{2C}^2$	$7.03 \delta x_{1F}^2 + 9.83 \delta y_{1F}^2 - 16.9 \delta z_{1F}^2 + 9.17 \delta x_{2F}^2 + 11.9 \delta y_{2F}^2 - 21.0 \delta z_{2F}^2$
Nonlinear in velocity	$0.0879 \delta v_{x1C}^2 + 0.163 \delta v_{y1C}^2 - 0.251 \delta v_{z1C}^2 + 0.0762 \delta v_{x2C}^2 + 0.150 \delta v_{y2C}^2 - 0.226 \delta v_{z2C}^2$	$0.179 \delta v_{x1F}^2 + 0.257 \delta v_{y1F}^2 - 0.437 \delta v_{z1F}^2 + 0.281 \delta v_{x2F}^2 + 0.364 \delta v_{y2F}^2 - 0.644 \delta v_{z2F}^2$
Position-velocity cross term	$0.685 \delta v_{x1C} \delta x_{1C} + 1.45 \delta v_{y1C} \delta y_{1C} - 2.14 \delta v_{z1C} \delta z_{1C} + 1.11 \delta v_{x2C} \delta x_{2C} + 1.96 \delta v_{y2C} \delta y_{2C} - 3.07 \delta v_{z2C} \delta z_{2C}$	$2.25 \delta v_{x1F} \delta x_{1F} + 3.15 \delta v_{y1F} \delta y_{1F} - 5.40 \delta v_{z1F} \delta z_{1F} + 2.93 \delta v_{x2F} \delta x_{2F} + 3.80 \delta v_{y2F} \delta y_{2F} - 6.73 \delta v_{z2F} \delta z_{2F}$

TABLE V: The same as in Table I but for the source mass geometry shown in Fig. 5.

Term	$C$ -configuration	$F$ -configuration
$\phi_s^T(z_i, v_{zi}) / \Delta^2 \phi$	0.367, -0.355	-0.124, 0.154
Linear in position	$10^{-11} (3.88 \delta z_{1C} - 16.5 \delta z_{2C}) + 2.01 \cdot 10^0 \times [\Gamma_{E31}(\delta x_{1C} - \delta x_{2C}) + \Gamma_{E32}(\delta y_{1C} - \delta y_{2C})]$	$10^{-9} [-6.50 \delta z_{1F} - 7.40 \delta z_{2F}] - 2.01 \cdot 10^0 \times [\Gamma_{E31}(\delta x_{1F} - \delta x_{2F}) + \Gamma_{E32}(\delta y_{1F} - \delta y_{2F})]$
Linear in velocity	$10^{-12} (9.49 \delta v_{z1C} - 28.3 \delta v_{z2C}) + 4.89 \cdot 10^4 \times [\Gamma_{E31}(\delta v_{x1C} - \delta v_{x2C}) + \Gamma_{E32}(\delta v_{y1C} - \delta v_{y2C})]$	$10^{-9} [-1.58 \delta v_{z1F} - 1.76 \delta v_{z2F}] - 4.89 \cdot 10^4 \times [\Gamma_{E31}(\delta v_{x1F} - \delta v_{x2F}) + \Gamma_{E32}(\delta v_{y1F} - \delta v_{y2F})]$
Nonlinear in position	$3.22 \delta x_{1C}^2 + 3.21 \delta y_{1C}^2 - 6.43 \delta z_{1C}^2 + 3.62 \delta x_{2C}^2 + 3.61 \delta y_{2C}^2 - 7.24 \delta z_{2C}^2$	$3.45 (\delta x_{1F}^2 + \delta y_{1F}^2) - 6.90 \delta z_{1F}^2 + 3.80 (\delta x_{2F}^2 + \delta y_{2F}^2) - 7.60 \delta z_{2F}^2$
Nonlinear in velocity	$0.212 \delta v_{x1C}^2 + 0.211 \delta v_{y1C}^2 - 0.423 \delta v_{z1C}^2 + 0.223 (\delta v_{x2C}^2 + \delta v_{y2C}^2) - 0.446 \delta v_{z2C}^2$	$0.209 (\delta v_{x1F}^2 + \delta v_{y1F}^2) - 0.418 \delta v_{z1F}^2 + 0.246 (\delta v_{x2F}^2 + \delta v_{y2F}^2) - 0.492 \delta v_{z2F}^2$
Position-velocity cross term	$1.56 (\delta v_{x1C} \delta x_{1C} + \delta v_{y1C} \delta y_{1C}) - 3.12 \delta v_{z1C} \delta z_{1C} + 1.76 (\delta v_{x2C} \delta x_{2C} + \delta v_{y2C} \delta y_{2C}) - 3.52 \delta v_{z2C} \delta z_{2C}$	$1.68 (\delta v_{x1F} \delta x_{1F} + \delta v_{y1F} \delta y_{1F}) - 3.35 \delta v_{z1F} \delta z_{1F} + 1.85 (\delta v_{x2F} \delta x_{2F} + \delta v_{y2F} \delta y_{2F}) - 3.69 \delta v_{z2F} \delta z_{2F}$